Comparative analysis of various statistical models for the identification Landslide Risk zone on Settlement and Roads in the East Sikkim Himalaya, India

Sk Asraful Alam (alamrsgis13@gmail.com)
Vidyasagar University
Ramkrishna Maiti
Vidyasagar University
Sujit Mandal
Diamond Harbour Women's University

Research Article

Keywords: Landslide susceptibility index, Landslide risk assessment, Success rate curve, landslide density, Receive operating curve

Posted Date: May 17th, 2022

DOI: https://doi.org/10.21203/rs.3.rs-1586666/v1

Abstract

Landslide is one the catastrophic event in Himalayan region. The settlement and roads are immensely affected by the landslide which is not only observed in east Sikkim Himalaya but also the entire mountain regions. The NH 31A road of East Sikkim Himalaya experiences numerous landslide events. The present objective of this study to embed various landslide Risk Assessment (LRA) models (Bivariate Statistical Index (BSI), Index of Entropy (IOE) and Weight of Evidence (WOE)) in the Rorachu watershed in the East Sikkim Himalaya and study the comparative analysis of this models. Firstly, the landslide inventory map was prepared by recent field survey study, aerial photograph and historical landslide records. There were 153 landslides locations which were mapped using GIS software and classified into 70% (107) for training the model of BSI, IOE and WOE and remaining 30% (46) were used for the validations. The 13 landslide causative factors were prepared as a database. Using these factors map the LSI and LRA maps were produced by BSI, IOE and WOE models. Finally, the LSI maps were validated by ROC curve, landslide density (LD) and success rate curve (SRC). The result shows that the LSI map using the WOE model is the highest prediction accuracy AUC = 0.858 (85.80%), followed by the BSI model (AUC = 0.858/85.80%) and IOE model (AUC = 0.687/68.70%). The LSI map using WOE model having the highest Success rate (SC) followed by BSI model and the IOE model. The results obtained from this study element-at-risk (Settlement and Road) which is revealed the LRA was shown that the highest risk of settlements areas by the model of BSI (40.32% areas), IOE (40.33% areas) and WOE (39.52% areas) and the highest risk of NH 31A road is BSI (40.04% areas), IOE (38.22% areas) and WOE (39.78% areas). This study has been identifying the maximum landslide risk areas of settlement and NH31A roads. The Bayesian weight of evidence (WOE) model is showing best fit to this study areas whereas index of entropy (IOE) and bivariate statistical index (BSI) showing comparatively low fit to this study. These landslide susceptibility map and landslide risk assessment (LRA) map can be used for the development of land use planning strategies, saves human loss and important for the planners and mitigation purpose.

Introduction

Climate change, urbanisation, and industrialization practices have all been quite efficient in raising the risk of landslides in hilly areas in recent years. Landslides cost developing countries 0.5 percent of their annual gross domestic product (GDP) and 95 percent of landslide-related inversions occur in developing countries (Chung et al. 1995). Because of its young mountain range with steep slopes, fragile geological formation, high intensity monsoonal rainfall, urbanisation, road construction, and deforestation, the Himalayan region is more geo-dynamically active, making Sikkim Himalaya more vulnerable and one of the world's most hazardous prone areas. Landslides are a more common natural disaster in mountainous places, when they have caused an unforeseen alteration in the earth's surface. Slope failure has been predicted to generate over $1 billion in damage in the Himalayan region each year, in addition to more than 200 casualties (Naithani 1999). Landslides have gotten a lot of attention recently, owing to a growing awareness of their socioeconomic impact and the increasing pressure of development on the mountain environment (Aleotti and Chowdhury 1999).

Landslide risk assessment (LRA) is one of the most important aspects of mountain development and management. The possibility of a hostile outcome, loss, harm, or damage to the human population and valuable belongings as a result of slope failure events is known as slope failure risk (Lee and Zones 2004). Landslides have become much more common in recent decades, highlighting the need of studying landslide susceptibility zonation (LSZ) mapping as well as landslide risk assessment (LRA) mapping for management and planning. The LSZ maps can also be generated using qualitative or quantitative methodologies (Soeters and van Westen 1996; Aleotti and Chowdhury 1999). Furthermore, the LSZ map is a critical component in LRA mapping. This information can be used to plan and

manage the Rorachu watershed in the Sikkim Himalaya. The spatial possibility of a landslide instance has been considered in the present context as landslide susceptibility zonation and the vulnerability of the element-at-risk. The LRA is determined by two factors: the likelihood of a landslide emerging in this field and the vulnerability of the element at risk.

The Sikkim Himalaya is one of the Himalayan range's most landslide-prone locations. As a result, the development of a landslide susceptibility zonation (LSZ) map and a landslide risk assessment (LRA) is critical for planning and development. Landslide susceptibility zone (LSZ) and landslide risk mapping can be done using a variety of qualitative and quantitative models. Several research on landslide susceptibility zonation utilising GIS have been conducted over the years (Akgun et al. 2008; Wan and Lei 2009; Wan et al. 2009; Akgun and Needet 2010; Pradhan and Youssef, 2010; Pradhan et al. 2011, 2012; Bednarik et al. 2012). For landslide hazard and risk zonation mapping, a variety of statistical models have been applied. Landslides have long been a concern in the Rorachu watershed in east Sikkim. The current study uses three statistical models (IOE, WOE, and BSI) to create landslide susceptibility and risk maps again for Rorachu watershed in the South Sikkim Himalaya. Various scholars have employed the bivariate statistical index (BSI) model, notably Westen V. et al. 1997; Rautela and Lakhera 2000; Cevik and Topal 2003; Regmi et al. 2013. Oh and Lee 2011; Dahal et al. 2008b; Singh et al. 2005; Lee and Choi 2004; Ma et al. 2019 use the weight of evidence (WOE) method, which was used for landslide susceptibility and risk zonation mapping by Oh and Lee 2011; Dahal et al. 2008b; Singh et al., 2005; Lee and Choi 2004; Ma et al. 2019. Constantin et al. 2011; Devkota et al. 2012; Jaafari et al. 2014; Youssef et al. 2014a; Pourghasemi et al. 2013b effectively implemented the index of entropy (IOE) model based on bivariate statistical analysis for landslide hazard zonation mapping. For the landslide susceptibility zonation (LSZ) and landslide risk assessment (LSA) of the Rorachu watershed of east Sikkim Himalaya, bivariate statistical index (BSI), Index of entropy (IOE), and Weight of evidence (WOE) models were used. The goal of this research was to forecast landslide susceptibility and danger. The goal of this study is to pinpoint the at-risk road and settlement zones. All models' performance was evaluated using established accuracy measures such as the Receive operation curve (ROC), Landslide density (LD), and Success rate curve (SRC).

The Study area

The study area is located in the east Sikkim district of Sikkim Himalaya. The Rorachu watershed bounded by $27^0$17’14.67” N to $27^0$23’48.50” N latitudes and $88^0$35’51.40” E to $88^0$43’11.98” E longitudes covering an area of around 69.125 km^2 (Figure 1). High relative reliefs, Steep slope along with immensely rugged surfaces are significant physiographic characteristics that makes superfluous landslide vulnerability in East Sikkim Himalaya. The settlement and roads are enormously affected by landslide in this zone. Rorachu watershed is one of them which is enormously affected by landslide. Therefore, the Rorachu watershed has been considered for research to identify landslide risk zones to population and roads areas. The maximum and minimum elevation of this Rorachu watershed is 4100 and 816 m respectively. The altitude of this watershed is highly diverse from southwestern periphery (Ranipool) to its northwestern boundary (Pandramaile). The Rorachu watershed feel like tranquil temperature throughout the year with an average maximum temperature 21^0 C during summer session and average minimum temperature 1^0C during winter session. The slope angle varies from 0^0 to as much as 71^0. The important town of this study area are Gangtok and Tadong whereas Samdong, Ranipool, Deorali are the main small markets. The area is undergoing fast development to urbanization in surrounding Gangtok and Ranipool town. Many local roads and highways (NH 31A) going through this watershed areas and new roads are also going to be constructed. The Rorachu watershed areas are mostly covered by forest, rocky and barren land, cultivated area and settlements. The physiographic and climatic diversity of this Rorachu watershed and fast developments are increasing the rate of slope instability. Along with this

climate change, uncertain rainfall and urbanization in Rorachu watershed is also impacting landslide hazards and Figure 1. Location map of the study area

risk.

Materials And Methods

In the present study, thirteen landslide causative factors i.e. Elevation, Geology, Slope, Soil, Drainage Density (DD), Road Density (RD), Rainfall, Normalize Difference Vegetation Index (NDVI), and Aspect, Topographic Position Index (TPI), Stream Power Index (SPI), Topographic Wetness Index (TWI) and Land Use Land Cover (LULC) were considered for performing landslide susceptibility Index (LSI) and landslide risk (LRA) modeling. Thus, this is important to compile a digitized database for executing the landslide susceptibility model and landslide risk model using geospatial techniques. The spatial databases have been designed and executed properly for the landslide vulnerability and landslide risk modeling (Table 2). In this study, both categorical and continuous data were used to perform landslide modeling with the help of ArcGIS 10.2, SPSS 23 and R software.

Table 1
Description of geological parameters of Rorachu watershed

ERA	FORMATION	CHARACTERISTICS	LITHOLOGY
Meso-Proterozoic	Lingtse gneiss	The gneisses are sheet like bodies of coarse to medium grained, foliated to strongly lineated granite mylonite. These are streaky, banded, augen gneisses or porphyroblastic gneisses and are traversed by concordant and discordant pegmatite veins. Amphibolite intrusives with sharp contacts are also recorded within gneisses. The most characteristic feature of the Lingtse granite is the presence of a stretching lineation.	Granite gneiss (mylonite)
Proterozoic (Undifferentiated)	Basic intrusive	Basic Intrusive rocks are characterized by large crystal sizes, and as the individual crystals are visible, the rock is called phaneritic. This is formed as the magma cools underground and while cooling may be fast or slow; cooling is slower than on the surface, so larger crystals grow.	Tourmaline / biotite leuco granite, schroll rock/ pegmatite, aplite (Undifferentiated)
	Gorubathan formation	The formation consists of mappable, monotonous sequence of inter banded chlorite sericite schist / phyllite, quartzite, meta greywacke, pyritiferrous black slate/ carbon phylllite, basic meta volcanics. Chlorite phyllite is dark green to light green whereas the quartz chlorite phyllite is only light green in color.	Interbanded chlorite-sericite schist / phyllite and quartzite, meta-greywacke (quartzo feldspathic greywacke), pyritiferous black slate, biotite phyllite / mica schist, biotite quartzite, mica schist with garnet, with / without staurolite, chlorite quartzite
	Kanchenjunga gneiss/Darjeeling gneiss	The gneisses, dominantly comprising quartz, feldspar and biotite (with minor amounts of other minerals) have been classified into three types, ie.1) banded / streaky gneisses / migmatites, 2) augen bearing biotite gneiss with/without garnet, kyanite, sillimanite and 3) sillimanite granite gneisses. Mapping of these rocks as individual units is very difficult because they are characterized by frequent interchanging and gradational features among themselves.	Banded / streaky migmatite, augen bearing (garnet) biotite gneiss with/ without kyanite, sillimanlte with palaeosomes of staurolite, kyanite, mica schist, biotite gneiss, sillimanite granite gneiss

ERA	FORMATION	CHARACTERISTICS	LITHOLOGY
	Chungthang formation	The main rock types of this formation are quartzites, garnet-kyanite-staurolite bearing biotite schist, calc silicate rock, graphitic schist and amphibolite.	Quartzite 2. Garnet kyanite sillimanite biotite schist / Garnetiferous mica schist Chungthang 3. Calc-silicate, carbonaceous schist Formation

Table 2
Sources of data layers of various landslide causative factors

Feature layer	Source	Thematic data layer	Resolution
Topographical map	Survey of India, Kolkata. Map no. 78A/11,	Drainage Density	1:50,000
Google Earth image	http://www.earth.google.com	Road Density	30 * 30 m
Geological map	Geological survey of India (GSI)	Geological map	1:250,000
Soil map	NBSS & LUP Regional Centre, Kolkata	Soil map	1:400,000
LANDSAT 8 OLI	http://www.earthexplorer.usgs.gov	Land Use Land Cover (LULC) map NDVI map	30 * 30 m 30 * 30 m
Rainfall data	http://www.worldclim.org	Rainfall Distribution map	1 km * 1 km
ASTER GDEM	http://www.earthexplorer.usgs.gov	Elevation map Slope map Topographic Wetness Index(TWI) map Topographic Position Index(TPI) map Stream Power Index(SPI) map	30 * 30 m 30 * 30 m 30 * 30 m 30 * 30 m 30 * 30m
Topographical map, Google earth image, Satellite data and GPS survey	Field study using GPS and internet	Landslide Inventory map	

3.1 Landslide inventory map

The essential part of the landslide vulnerability studies to ascertain the landslide inventory (Guzzetti et al. 1999). The landslide inventory map provide primary information for the evaluation of landslide hazard assessment and landslide risk assessment. Accurate detection and identification of landslide is most significant for probabilistic landslide susceptibility and landslide risk analysis (Rawat and Joshi 2016; Mondal and Mandal 2017a). The Landslide inventory map was made analyzing aerial photographs, LANDSAT 8 OLI (30 m) image, Google Earth (Quickbird image, 0.60 m) and GPS survey, and also include recent landslide locations in this study. Finally, all the data were vectorized in ArcGIS 10.3 software. In total 153 major and minor landslides were identified in the Rorachu watershed that have been showing the total areal coverage of 0.644 sq. km (Fig. 2). All the landslides data has been converted vector to raster format for the landslide susceptibility and landslide risk modelling. About 107 landslides areas (70%) out of the 153 areas were randomly selected for the model training, and remaining 46 landslide areas (30%) were used for the model validation purpose. Most of the landslides in this Rorachu watershed areas are rock slide, debris slide and earth slide.

3.2 Selection of Landslide conditioning factors

There is no such criteria for selecting causative factors for landslide vulnerability analysis (Ayalew and Yamagishi 2005). The factors controlling slope instability modeling and risk modelling are elevation, geology, slope, soil, drainage density (DD), road density (RD), Rainfall, Normalize Difference Vegetation Index (NDVI), and slope aspect, topographic position index (TPI), stream power index (SPI), topographic wetness index (TWI) and land use land cover (LULC). All these landslide causative variables are being used by different researcher in across the globe (Wu et al. 2017).

3.2.1 Geology, elevation, slope, soil and drainage density

The geology plays a significant preface in the occurrence of the slope instability because of the lithological and structural variations often leads to difference in strength of soil and rocks (Pradhan and Lee 2010a) in Rorachu watershed. Rorachu watershed areas are characterized by the presence of five lithological units i.e. 1. Basic Intrusive, 2. Chungthang Formation, 3.Gorubathan Formation, 4. Lingtse Gnesis, 5. Kanchenjunga Gnesis or Darjeeling Gnesis (undifferentiated) (Fig. 4 and Table 2). The geology map of Rorachu watershed was made using district resource map of east Sikkim which was collected from geological survey of india (GSI), Kolkata. Major part of this watershed is encircled by Kanchenjunga Gnesis or Darjeeling Gnesis. Lithological unit of basic Kanchenjunga gnesis covering large area (43.02%) and ranked first which is followed by Basic intrusive (21.10%), Chungthang formation (18.48%), Gorubathan formation (12.12%) and Lingtse Gnesis (5.35%). Due to different sets of structural disturbance, numerous fractures, faults, cracks and joints landslide activities are common in Sikkim Himalaya. The lithological characteristics influence stability of rocks and occurrences of landslide.

Elevation or altitude is one of the significant parameter that has been frequently used for landslide susceptibility and landslide risk modelling. Elevation control the another landslide occurrences parameter in a geographical area. It is controlled by various geological and geomorphological process (Ayalew et al. 2005; Pourghasemi 2008). In this present study area, the elevation ranges between 816 m and 4100 m (Fig. 4a). The elevation map is classified into 5 categories with 30 * 30 meter resolution. It has been noticed that maximum landslides are being observed in the medium and high elevation zones of the Rorachu watershed.

Slope gradient is also another significant causative factors of slope stability assessment (Lee and Min 2001). Stability of the slope is the interaction between angel of the slope and materials properties of the slope (friction angel, cohesion, porosity, permeability and bonding). Gentle slopes have minor probability for slope instability due to lower shear stress (Dai et al. 2001). In contrast, higher the slope gradient higher the shear stresses and vice versa. In this

present study slope map is classified into five categories using natural breaks method in ArcGIS 10.3. Slope angel ranges from 0^0 to 70^o (Fig. 4b) and there are more than 30% areas under 35^o to 70^o slope angel in this Rorachu watershed.

The *soil* saturation depends on two factors i.e. intensity, duration and amount of precipitation of this area and soil physical characteristics like, soil texture, structure, porosity, permeability, compactness etc. In Rorachu watershed more than 90% area is under hilly region. Soil areas of the Rorachu watershed have been seprated into six categories (Fig. 5. c, Table 3) such as I. coarse loamy humic dystrudepts, II. Coarse loamy humic lithic dystrudepts, III. Coarse loamy typic hapludolls, IV. Fine loamy fluventic eutrudepts, V. Fine skeletal cumuli hapludolls and VI. Loamy skeletal entic hapludolls. In Rorachu watershed, all soil categories have been converted into vector polygon and then to raster format (30 *30 meter grid).

Table 3
Description of soil parameters in the Rorachu watershed

Mapping unit	Soil name	Soil code	characteristics
Inceptisols	Coarse loamy humic dystrudepts	S001	Very deep, well drained, moderately rapid permeable coarse loamy soil is found in structural benches and Foot slope of mountain associated with moderately shallow to deep, little stony, excessively drained coarse loamy soil with moderate erosion
	Coarse loamy humic Pachic dystrudepts	S002	Moderately rapid permeability is occurred in upland slopes associated with moderately deep, well drained coarse loamy soil with medium run-off,, little stony, excessively drained fine loamy soils with moderate erosion
	Coarse loamy typic hapludolls	S003	Excessively drained, deep coarse loamy soil having little stoniness and slight to moderate erosion is found mainly in the ridges associated with moderate deep to deep coarse loamy soil with little stoniness and moderate erosion
	Fine-loamy fluventic eutrudepts	S004	moderate permeability with Moderately shallow to deep, well drained fine loamy soil is found in steep slope, moderately high saturated hydraulic conductivity and moderate erosion associated with very deep, well drained fine loamy upland soils
Mollisols	Fine-skeletal cumilic hapludolls	S005	Moderately deep to very deep, excessively drained soils with gravelly surface, little stoniness and moderate erosion is found in very steep slope associated with moderately shallow to deep, slight stoniness, excessively drained, moderately erosion prone coarse loamy soil
	Loamy skeletal entic hapludolls	S006	Excessively drained, gravelly loamy soil mainly found in very steep hill side with small stoniness and moderate erosion associated with moderately shallow to deep, slight stoniness, moderately deep to deep, excessively drained, moderately erosion prone gravelly loamy soil

Drainage density is the total length of all streams and rivers of that grid divided by the total area (Eq. 1) of that grid (Horton 1932, 1945; Strahler 1952). Drainage density (DD) indicates the measure of how enough or how unwell a river watershed is drained by the stream channels. Drainage density depends on both physical environment and climatic

environments of an area. Drainage density helps to determine the degree of reducing the shear strength of mountain slope which has affective role in slope instability. Drainage density of Rorachu river basin has been made using Euclidean distance method in ArcGIS 10.3 into 30 * 30 meter grid (Fig. 4d) and classified into five by natural breaking method.

$$Dd = (Lt/Abasin)$$

1

Where, D_d represents drainage density, L_T represents total length of the streams in that grid and A_{basin} represents total length of the grid area.

3.2.2 Road density, Normalized Difference vegetation Index (NDVI), Slope Aspect, Topographic position index (TPI)

The high *road density* reduces the strength of soil and slope which invites landslide. All the anthropogenic activities i.e. construction and extension of road networks are responsible for slope instability. Roads modify the inherent gradient of the slope and generate an obstacle for the surface water flow (Marcini 2010). Road map was made using Topographical map and Google Earth. In this Rorachu watershed area, road density was prepared by ArcGIS 10.3 into 30 * 30 meter grid cell (Fig. 5e) and then it has been classified into five groups.

Normalized difference vegetation index (NDVI) is a numerical indicator that uses for the vegetation conditions of the surface. NDVI has been estimated by the formula of NDVI = {(NIR − R) / (NIR + R)}, where NIR is the Near Infrared band and R is the Red band of satellite image. In Rorachu watershed, NDVI was assessed incorporating LANDSAT 8 OLI image in ERDAS 9.2 image processing software (Fig. 6. f) where NDVI value ranges from − 0.11 to 0.64. Positive value indicates the healthy vegetation cover which increase soil cohesion and slope stability. A negative NDVI value indicates no vegetation cover in Rorachu watershed areas which is more vulnerable for soil erosion and slope failure.

The *Slope aspects* are the compass direction of maximum slope faces of the terrain surface. The direction of the slope faces can affect physical and biological factors which are related to landslide hazards. Slope aspects are immensely influence on temperature and vegetation cover. The slope aspect map has been prepared from the DEM. The slope aspects are connected to the physiographic aptitude and the principle precipitation direction (Ercanoglu and Gokceoglu 2002). In this present study, the slope aspects are classified into ten categories (Flat, N, NE, E, SE, S, SW, W, NW, and N).

h. Topographic position index (TPI)

Topographic position index (TPI) is an algorithm which is immensely used to measure topographic slope positions and automated landform classifications. The topographic position index (TPI) refers to the topographic position classification identifying upper, middle and lower part of the landscape (Guisan et al. 1999). Positive TPI values have been representing the locations that are higher than the surroundings (ridges). Negative TPI values have been representing the locations that are lower than the surroundings (valleys). TPI values are close to zero have been representing either flat areas or a constant slope. In this study area, the TPI value was calculated by the SAGA GIS software, and the value of TPI ranges between the − 63.51 and 65.13. The Topographic position index is an important factor for the assessment of a landslide vulnerability and a landslide risk (Fig. 6. h).

3.2.3 Stream power index (SPI), Topographic Wetness Index (TWI), Land use Land cover (LULC) and rainfall

Stream power index (SPI) is quantifying the erosive power of the flowing water on a slope gradient. The stream power index (SPI) has been estimated based on the slope and specific catchment area (SCA). The stream power index (SPI) is defined after Moore and Grayson (1991) (Eq. 2).

$$\mathrm{SPI} = (\mathrm{As} \times \tan\beta)$$

2

Where, As is the specific catchment area (SCA) and β is the local slope gradient measured in degrees, respectively. In this Rorachu watershed, SPI values varies from 0 to 145.37 and the study area is classified into five classes (Fig. 7. i) after Hengl et al. (2003) (Eq. 3).

$$As = (Am \times P^2 / \sum Li)$$

3

In the above equation, P is the pixel size, Am is the cumulative drainage fraction from m neighbors, and ∑Li is derived as the sum of lengths for drainage pixels.

Topographic wetness index (TWI) is another important factors for landslide susceptibility and a risk modeling. TWI refers to the accumulation of water in a particular point of time to any grid cell. For shallow landslide modeling, TWI has been used by various researchers (Gokceoglu et al. 2005; and Yilmaz 2009a 2009b). In this study, TWI map was prepared by SAGA GIS software after Beven and Kirkby (1979). TWI map was classified into five categories (Fig. 7j). TWI is defined as:

$$\mathrm{TWI} = \ln\left(\frac{\mathrm{a}}{\tan\beta}\right)$$

4

Where, a is the cumulative upslope area draining through a point (per unit contour length) and tanβ is the slope angel at that point.

LULC map was prepared from the LANDSAT 8 OLI satellite image (2019) data, using supervised classification techniques in ERDAS 9.2 software. The forest area promotes infiltration and drainage which reduces the slope failure. The slope stability is affected by the cultivated lands (Devkota et al. 2012). The study area exhibits various types of land use land cover such as step cultivation, open forest, settlement, bare soil, landslide area, river and dense forest. In this Rorachu watershed most of the area covered by the forest (open and dense, 59%) which is followed by the settlement (3.47%) and bare land (3.23%) (Fig. 7. L, Table 4.).

Table 4
Landslide causative factors and their sub-class for landslide susceptibility and Landslide risk mapping

Factors	Sub-Class
Elevation	816–1495, 1495–1993, 1993–2516, 2516–3110, 3110–4100
Slope	0–15.37, 15.37–25.53, 25.53–35.14, 35.14–45.57, 45.57–70.01
Soil	S001, S002, S003, S004, S005, S006
Drainage Density (DD)	0.092–2.17, 2.17–3.62, 3.62–4.92, 4.92–6.25, 6.25–9.557
Geology	Basic intrusive, Chungthang formation, Gorubathan formation, Lingtse gnesis, Kanchenjunga gnesis/Darjeeling gnesis (undifferential)
Road Density (RD)	0–0.88, 0.88–2.55, 2.55–4.48, 4.48–6.86, 6.86–11.175
Normalize Difference Vegetation Index (NDVI)	-0.11–0.14, 0.14–0.24, 0.24–0.34, 0.34–0.43, 0.43–0.642
Aspect	Flat, North, Northeast, East, Southeast, South, Southwest, West, Northwest
Topographic Position Index (TPI)	-63.51 - -14.57, -14.57 - -4.48, -4.48–4.59, 4.59–15.18, 15.18–65.135
Stream Power Index (SPI)	0–2.85, 2.85–9.12, 9.12–20.52, 20.52–47.88, 47.88–145.37
Topographic Wetness Index (TWI)	5.83–8.31, 8.31–9.19, 9.19–10.15, 10.15–11.26, 11.26–15.25
Land Use Land Cover (LULC)	Step cultivation. Open forest, Settlement, Bare soil, Landslide area, River, Dense forest
Rainfall	1874.47–2386.86, 2386.86–2791.41, 2791.41–3096.59, 3096.59–3323.70, 3323.70–3657.28

Table 5
Monthly Rainfall distribution in the East Sikkim area (2009–2015).

Source: Indian Meteorological Department (IMD) Gangtok, Sikkim

Year	Jan	Feb	Mar	Apr	May	June	July	Aug	Sep	Oct	Nov	Dec
2009	5.7	4.2	87.3	251.7	335.4	355.4	408.6	454.1	180.1	201.6	1.7	5.4
2010	5.7	18	187	359.4	272.7	504.6	601	493.8	375.8	95.6	23.6	0.1
2011	21.6	40.5	68.5	14.7	278.8	515.9	587.3	459.1	376.7	44.9	60.8	2.3
2012	17.8	21.5	28.4	312.2	201.6	614.4	481.3	442.2	410.9	72.4	0.1	1
2013	4.3	32.1	128	256.1	409	382.6	412.1	325.1	195.5	191.8	40.7	7.9
2014	0	5.4	68.2	96.1	441.4	472.7	478.7	522.3	273	16.7	2.4	4.2
2015	7.4	17.4	73.3	270.3	387.8	603.1	561	284.7	316.1	99.6	55.8	1

Rainfall is one of the most significant triggering factors for landslides events in Rorachu watershed. The Rainfall map was prepared using world climatic data and applying inverse distance weighted (IDW) modeling and then classified

into 5 categories. Rainfall in Rorachu watershed ranges between 1847 mm and 3657 mm. Maximum rainfall occurs between June and August (According to IMD data, Table 5. and Figure 7. m).

3.3 Modelling landslide susceptibility and Risk

3.3.1 Application of Bivariate Statistical index (BSI) model

The bivariate statistical index (BSI) model is used for the landslide susceptibility and landslide risk assessment modelling in Rorachu watershed (Table 6). The statistical index (SI) model is a bivariate statistical approach which has been used by van Westen (1997) for the landslide susceptibility modelling. In recent years the bivariate statistical index (BSI) model is widely used by different researcher for the landslide susceptibility and landslide risk modelling. In bivariate statistical index (BSI) model, a weighted value for every categorical units are defined as the natural logarithm of the landslide density in the categorical unit divided by the landslide density in the entire study area (van Westen 1997; Rautela and Lakhera 2000; Cevik and Topal 2003). This bivariate statistical index (SI) approach is based on this following equation (van Westen 1997).

Table 6
Spatial relationship between each landslide conditioning factors and observed landslides Using Bivariate Statistical Index (BSI) and Weight of Evidence (WOE) models.

Factors	Class	Class pixel	Landslide pixel	W+	W-	C	BSI
Elevation (m)	4100–3110	6841	218	1.23	-0.27	1.50	1.23
	3110–2516	16104	338	0.81	-0.40	1.22	0.81
	2516–1993	20031	139	-0.30	0.09	-0.38	-0.30
	1993–1495	19285	16	-2.42	0.27	-2.69	-2.42
	1495 – 816	14545	5	-3.30	0.20	-3.50	-3.30
Geology	Gorubathan formation	9312	6	-2.67	0.12	-2.79	-2.67
	Lingtse genesis	4112	0	0	0.06	-0.06	0
	Basic intrusive	16210	54	-1.03	0.16	-1.19	-1.03
	Chungthang formation	14123	255	0.66	-0.24	0.90	0.66
	Kanchenjunga formation	33049	401	0.26	-0.26	0.52	0.26
Slope (^{o})	70.09–45.57	7799	114	0.45	-0.07	0.52	0.45
	45.57–35.14	15677	210	0.36	-0.12	0.48	0.36
	35.14–25.53	20253	218	0.14	-0.06	0.20	0.14
	25.53–15.37	20229	126	-0.40	0.11	-0.52	-0.40
	15.37–0	12848	48	-0.91	0.11	-1.03	-0.91
Soil	Fine skeletal	5224	1	-3.89	0.07	-3.95	-3.89
	Coarse loamy distrudeptic	32878	127	-0.88	0.36	-1.24	-0.88
	Coarse loamy holithic	11997	156	0.33	-0.08	0.41	0.33
	Fine loamy	6534	0	0.00	0.09	-0.09	0
	Loamy skeletal	3754	126	1.28	-0.14	1.42	1.28
	Coarce loamy	16419	306	0.69	-0.32	1.01	0.69
Drainage Density	9.55–6.25	12033	62	-0.59	0.08	-0.67	-0.59
	6.25–4.92	18190	73	-0.84	0.16	-1.01	-0.84
	4.92–3.62	17869	140	-0.17	0.05	-0.22	-0.17
	3.62–2.17	16626	312	0.70	-0.33	1.03	0.70
	2.17–0.09	12088	129	0.14	-0.03	0.16	0.14

(NDVI = Normalize Difference Vegetation Index, TWI = Topographic Wetness Index, SPI = Stream Power Index, TPI = Topographic Position Index and LULC = Land Use Land Cover)

Factors	Class	Class pixel	Landslide pixel	W+	W-	C	BSI
Road Density	11.17–6.86	2051	13	-0.39	0.01	-0.39	-0.39
	6.86–4.48	4530	100	0.86	-0.09	0.95	0.86
	4.48–2.55	8439	252	1.16	-0.32	1.48	1.16
	2.55–0.88	14317	157	0.16	-0.04	0.20	0.16
	0.88–0	47469	194	-0.82	0.65	-1.47	-0.82
Rainfall (mm)	1847–2386	6624	263	1.45	-0.37	1.82	1.45
	2386–2791	5199	95	0.67	-0.07	0.75	0.67
	2791–3096	12076	137	0.20	-0.04	0.24	0.20
	3096–3323	31797	195	-0.42	0.22	-0.64	-0.42
	3323–3657	21110	26	-2.02	0.28	-2.31	-2.02
TPI	15.25–11.26	6669	67	0.07	-0.01	0.08	0.07
	11.26–10.15	18765	173	-0.01	0.00	-0.01	-0.01
	10.15–9.19	25823	228	-0.05	0.03	-0.08	-0.05
	9.19–8.31	18956	171	-0.03	0.01	-0.04	-0.03
	8.31–5.83	6593	77	0.23	-0.02	0.25	0.23
SPI	145.37–47.88	133	0	0	0.00	0.00	0
	47.88–20.52	1060	7	-0.34	0.00	-0.35	-0.34
	20.52–9.12	4966	57	0.21	-0.02	0.22	0.21
	9.12–2.85	21030	255	0.26	-0.12	0.38	0.26
	2.85–0	49617	397	-0.15	0.23	-0.38	-0.15
TWI	65.13–15.18	5334	20	-0.91	0.04	-0.95	-0.91
	15.18–4.59	13142	65	-0.63	0.09	-0.73	-0.63
	4.59 - – 4.48	21264	206	0.04	-0.02	0.05	0.04
	-4.48 - – 14.57	22952	263	0.21	-0.10	0.31	0.21
	-14.57 - – 63.51	14114	162	0.21	-0.05	0.26	0.21
LULC	Step cultivation	1648	0	0	0.02	-0.02	0
	dense forest	45962	309	-0.33	0.35	-0.67	-0.33
	settlement	3865	7	-1.64	0.04	-1.68	-1.64
	bare soil	3921	149	1.41	-0.18	1.59	1.41

(NDVI = Normalize Difference Vegetation Index, TWI = Topographic Wetness Index, SPI = Stream Power Index, TPI = Topographic Position Index and LULC = Land Use Land Cover)

Factors	Class	Class pixel	Landslide pixel	W+	W-	C	BSI
	river	1439	0	0	0.02	-0.02	0
	open forest	19971	251	0.30	-0.13	0.43	0.30
Aspect	Flat	4	0	0	5E-05	-5E-05	0
	North	2614	0	0	3E-02	-3E-02	0
	Northeast	2042	5	-1.34	0.02	-1.36	-1.34
	East	5587	52	0.00	0.00	0.00	0.00
	Southeast	10496	137	0.34	-0.07	0.40	0.34
	South	14015	174	0.29	-0.08	0.36	0.29
	Southwest	10206	207	0.76	-0.19	0.96	0.76
	West	12646	116	-0.02	0.00	-0.02	-0.02
	Northwest	14206	28	-1.55	0.16	-1.72	-1.55
	North	4990	0	0	0.07	-0.07	0
NDVI	0.64–0.43	9717	205	0.21	-0.06	0.26	0.82
	0.43–0.33	13283	160	-0.78	0.19	-0.97	0.26
	0.33–0.24	17463	90	-0.59	0.12	-0.72	-0.59
	0.24–0.14	21584	92	0.26	-0.06	0.32	-0.78
	0.14 – 0.11	14759	169	0.82	-0.20	1.02	0.21

(NDVI = Normalize Difference Vegetation Index, TWI = Topographic Wetness Index, SPI = Stream Power Index, TPI = Topographic Position Index and LULC = Land Use Land Cover)

$$W_{BSI} = \ln\left(\frac{Eij}{E}\right) \quad (5)$$

$$W_{BSI} = ln\left[\frac{N(Si)}{N(Ni)} / \frac{?N(Si)}{?N(Ni)}\right] \quad (6)$$

Where, W_{BSI}, weight given to a certain class i of parameter j; Eij, landslide density within class i of parameter j; E, total landslide density within the entire study area. Here N (Si) is the number of landslide pixels in parameter class i, and N (Ni) is the total number of pixels in the same parameter class. In this current research every landslide causative factors were crossed checked with this landslide inventory map for determining the density of landslide for every class. The ultimate landslide susceptibility and risk map was produced in ArcGIS raster calculator tool. Positive W_{BSI} values indicates the significant relationship within landslide causative variables and distribution of landslides. The negative W_{BSI} values indicate the relationship between landslide causative factors and distribution of landslides are not relevant. In this study, the final landslide susceptibility index (LSI) map (Fig. 8) was prepared by bivariate statistical index (BSI) model (Eq. 7).

LSI_{BSI} = ((W_{BSI} * Elevation) + (W_{BSI} * Slope) + (W_{BSI} * Aspect) + (W_{BSI} * Geology) +
(W_{BSI} * Soil) + (W_{BSI} * Drainage density) + (W_{BSI} * Road density) + (7)

(W_{BSI} * Rainfall) + (W_{BSI} * TWI) + (W_{BSI} * SPI) +

(W_{BSI} * TPI) + (W_{BSI} * NDVI) + (W_{BSI} * LULC))

3.3.2 Weight of evidence (WOE) model

The WOE model is a bivariate statistical method based on the Bayesian approach and this was primary accomplish for non-spatial and quantitative imposition in the medical sciences (Lusted 1968). Thus, this success was extensively consecrated and acknowledgement on the geosciences for mineral potential mapping (Bonham-Carter et al., 1988), and ultimately applied in Slope instability and hazard mapping by different scholar (Lee et al. 2002a, b; van Westen et al. 2003; Mathew et al. 2007; Dahal et al. 2008a, b; Regmi et al. 2010). Weight of evidence (WOE) is a Bayesian approach with log-linear form which is uses preceding probability and subsequent probability (Regmi et al. 2010a). Previously, Van Western (2002) applied the method for landslide susceptibility assessment. This model is based on a log-linear form of Bayesian rule and can be written as:

$$P(A \mid B) = \frac{P(B \mid A) \times P(A)}{P(B)}$$

8

Thus, the probability of several events A occurring, given that event B has already occurred, P(A|B), is equal to the probability of event B taking place that event A has occurred, P(B|A), multiplied by the probability of event A occurring, P(A), and divided by the probability of event B occurring, P(B). WOE model calculates the weight of each landslide predictive factor (B) based on the degree of connection in the presence or absence of the landslide (L) within the area, (Bonham-Carter, 1994) as follows:

$$Wi^{+} = \ln \frac{P\{B \mid A\}}{P\left\{B \mid \bar{A}\right\}}$$

9

$$Wi^{+} = \ln \left\{ \frac{(Npix1 \,/\, (Npix1 + Npix2))}{(Npix3 \,/\, (Npix3 + Npix4))} \right\}$$

10

$$Wi^{-} = \ln \frac{P\left\{\bar{B} \mid A\right\}}{P\left\{\bar{B} \mid \bar{A}\right\}}$$

11

$$Wi^{-} = \ln\left\{\frac{(Npix2\,/\,(Npix1 + Npix2))}{(Npix4\,/\,(Npix3 + Npix4))}\right\}$$

12

Where, P is the probability and *ln* is the natural log. Similarly, B is the availability of possible landslide predictive factor, $\bar{B}$ is the absence of a potential landslide predictive factor, A is the presence of landslide, and Ā is the absence of a landslide. The positive weight (Wi^{+}) introduced that the predictable variable is present at the landslide locations in the sub-category factors and augmentation of this weight is an indication of positive correlation between predictable variables and landslides. The negative weight (Wi^{-}) indicates the absence of the predictable variable and shows the level of negative correlation (Dahal et al. 2008a). The difference between two weights is called weighted contrast (C, EQ. 19). The final landslide susceptibility index (LSI) is produced by the combination of each landslide causative factors using overlay methods (Eq. 14).

$$C = (Wi^{+} - Wi^{-})$$

13

$$LSI = \sum_{i=1}^{N} C$$

14

Applying bivariate WOE statistical model the landslide susceptibility index (LSI) map was made (Eq. 15).

LSI_{WOE} = ((W_{WOE} * Elevation) + (W_{WOE} * Slope) + (W_{WOE} * Aspect) +

(W_{WOE} * Geology) + (W_{WOE} * Soil) + (W_{WOE} * Drainage density) + (15)

(W_{WOE} * Road density) + (W_{WOE} * Rainfall) + (W_{WOE} * TWI) +

(W_{WOE} * SPI) + (W_{WOE} * TPI) + (W_{WOE} * NDVI) + (W_{WOE} * LULC))

3.3.3 Application of Index of Entropy (IOE) model

The index of entropy (IOE) model computes the weight of all landslides causative factors based by the bivariate analysis approach and used for determine the landslide susceptibility and landslide risk. The entropy by Shannon (1948) which is based on measured of uncertainty amalgamated with a random variable, imitating the system information content. Imbalance, disorder, uncertainty and instability of a systems are determined based on entropy (Yufeng and Fengxiang 2009). In this IOE model, the weighting process is based on this methodology which is proposed by Vlcko et al. (1980). The index of entropy (IOE) is widely used model and that determine the weight index of natural hazards and has been used various environmental impact assessment modelling, such as sand storms, droughts, debris flows and landslides (Li et al., 2002; Mon et al. 1994; Ren, 2000; Yi and Shi, 1994; Yang and Qiao 2009; Devkota et al. 2013; Jaafari et al. 2014; Youssef et al., 2014a, b). In the present study, the weighted parameter was obtained from the defined level of entropy representing the boundary where various factors influence the development of a landslide susceptibility and landslide risk. The information coefficient Wj representing the weight value for the causative factors and, it was calculated after Bednarik et al. (2010) and Constantin et al. (2011) which are as follows.

$$Pij = \frac{b}{a},$$

16

$$(Pij) = \frac{Pij}{? \sum_{j=1}^{Sj} Pij},$$

17

Here, Hj and Hjmax are the entropy values (Eq. 16, 17) and they are written as;

$$Hj = - ? \sum_{i=1}^{Sj} (Pij) log2(Pij), j = 1, 2, \ldots, n,$$

18

$Hjmax = log2Sj,$ Sj is the number of classes (19)

Ij is the information coefficient (Eq. 20) and Wj narrate the resultant weight value for the landslide causative parameter as a whole (Eq. 21).

$Ij = \frac{Hj\max - Hj}{Hjmax}$ I = (0, 1) j = 1, 2.. . n, (20)

$$Wj = Ij \times Pj$$

21

Where a and b are the domain and landslide percentages, respectively (Pij) is the probability density. The result ranges from 0 to 1. The closer the value of 1, the greater the slope instability and vice versa. The complete calculation of weight determination for the individual landslide causative parameters is presented in Table 7. The ultimate landslide susceptibility map was prepared by the summation of all individual landslide causative parameter classes. The final landslide susceptibility map was prepared using by this following equation as follows:

Table 7
The spatial relationship between every landslide conditioning factors and observed landslides Using Index of Entropy (IOE) models for all landslide causative factors classes.

Factors	Class	Class pixel	Landslide pixel	P_{IJ}	(P_{IJ})	H_J	H_J max	I_J	P_J	W_{IJ}
Elevation (m)	4100–3110	6841	218	3.42	0.52	1.502	2.32	0.353	1.308	0.4617
	3110–2516	16104	338	2.25	0.34					
	2516–1993	20031	139	0.74	0.11					
	1993–1495	19285	16	0.09	0.01					
	1495 – 816	14545	5	0.04	0.01					
Geology	gorubathan formation	9312	6	0.07	0.02	1.45	2.32	0.375	0.773	0.2898
	lingtse genesis	4112	0	0	0.00					
	basic intrusive	16210	54	0.36	0.10					
	chungthang formation	14123	255	1.94	0.53					
	kanchanjangha formation	33049	401	1.30	0.36					
Slope (°)	70.09–45.57	7799	114	1.57	0.30	2.18	2.32	0.064	1.046	0.068
	45.57–35.14	15677	210	1.44	0.27					
	35.14–25.53	20253	218	1.15	0.22					
	25.53–15.37	20229	126	0.67	0.13					
	15.37–0	12848	48	0.40	0.08					
Soil	fine skeletal	5224	1	0.02	0.00	1.73	2.58	0.331	1.238	0.4097
	coarse loamy distrudeptic	32878	127	0.41	0.06					
	coarse loamy holithic	11997	156	1.39	0.19					
	fine loamy	6534	0	0	0.00					
	loamy skeletal	3754	126	3.60	0.48					
	coarce loamy	16419	306	2.00	0.27					
Drainage Density	9.55–6.25	12033	62	0.55	0.11	2.11	2.32	0.09	0.996	0.08964
	6.25–4.92	18190	73	0.43	0.09					
	4.92–3.62	17869	140	0.84	0.17					

(NDVI = Normalize Difference Vegetation Index, TWI = Topographic Wetness Index, SPI = Stream Power Index, TPI = Topographic Position Index and LULC = Land Use Land Cover)

Factors	Class	Class pixel	Landslide pixel	P_{IJ}	(P_{IJ})	H_J	H_J max	I_J	P_J	W_{IJ}
	3.62–2.17	16626	312	2.01	0.40					
	2.17–0.09	12088	129	1.14	0.23					
Road Density	11.17–6.86	2051	13	0.67	0.09	2.0	2.32	0.142	1.553	0.2204
	6.86–4.48	4530	100	2.33	0.30					
	4.48–2.55	8439	252	3.16	0.41					
	2.55–0.88	14317	157	1.16	0.15					
	0.88–0	47469	194	0.43	0.06					
Rainfall (mm)	1847–2386	6624	263	4.26	0.52	1.8	2.32	0.224	1.653	0.37054
	2386–2791	5199	95	1.96	0.24					
	2791–3096	12076	137	1.22	0.15					
	3096–3323	31797	195	0.66	0.08					
	3323–3657	21110	26	0.13	0.02					
TPI	15.25–11.26	6669	67	1.08	0.21	2.31	2.32	0.004	1.047	0.00418
	11.26–10.15	18765	173	0.99	0.19					
	10.15–9.19	25823	228	0.95	0.18					
	9.19–8.31	18956	171	0.97	0.18					
	8.31–5.83	6593	77	1.25	0.24					
SPI	145.37–47.88	133	0	0	0	1.96	2.32	0.159	0.819	0.1303
	47.88–20.52	1060	7	0.71	0.17					
	20.52–9.12	4966	57	1.23	0.30					
	9.12–2.85	21030	255	1.30	0.32					
	2.85–0	49617	397	0.86	0.21					
TWI	65.13–15.18	5334	20	0.40	0.09	2.20	2.32	0.056	0.884	0.0495
	15.18–4.59	13142	65	0.53	0.12					
	4.59 - – 4.48	21264	206	1.04	0.23					
	-4.48 - – 14.57	22952	263	1.23	0.28					
	-14.57 - – 63.51	14114	162	1.23	0.28					
LULC	Step cultivation	1648	0	0	0	1.40	2.81	0.504	1.056	0.53206

(NDVI = Normalize Difference Vegetation Index, TWI = Topographic Wetness Index, SPI = Stream Power Index, TPI = Topographic Position Index and LULC = Land Use Land Cover)

Factors	Class	Class pixel	Landslide pixel	P_{IJ}	(P_{IJ})	H_J	H_J max	I_J	P_J	W_{IJ}
	dense forest	45962	309	0.72	0.11					
	settlement	3865	7	0.19	0.03					
	bare soil	3921	149	4.08	0.64					
	river	1439	0	0	0.00					
	open forest	19971	251	1.35	0.21					
Aspect	Flat	4	0	0	0	2.54	3.32	0.235	0.733	0.17221
	North	2614	0	0	0					
	Northeast	2042	5	0.26	0.04					
	East	5587	52	1.00	0.14					
	Southeast	10496	137	1.40	0.19					
	South	14015	174	1.33	0.18					
	Southwest	10206	207	2.14	0.29					
	West	12646	116	0.98	0.13					
	Northwest	14206	28	0.21	0.03					
	North	4990	0	0	0					
NDVI	0.64–0.43	9717	205	2.26	0.39	2.11	2.32	0.091	1.158	0.1048
	0.43–0.33	13283	160	1.29	0.22					
	0.33–0.24	17463	90	0.55	0.10					
	0.24–0.14	21584	92	0.46	0.08					
	0.14 - – 0.11	14759	169	1.23	0.21					

(NDVI = Normalize Difference Vegetation Index, TWI = Topographic Wetness Index, SPI = Stream Power Index, TPI = Topographic Position Index and LULC = Land Use Land Cover)

$$YIOE = \sum_{i}^{n} \frac{z}{mi} \times C \times Wj,$$

22

Where *YI*OE is the aggregate of all the factors classes; *i* is the number of particular parametric map (1, 2,. . ., *n*); *z* is the number of classes within landslide parametric map with the greatest number of classes; *mi* is the number of classes within particular landslide parametric map; *C* is the value of the class after secondary classification and *Wj* is the weight of a parameter (Bednarik *et al.*2010; Devkota *et al.*2013; Jaafari *et al.*2014). Applying IOE approach, the landslide susceptibility index (LSI) map was made for the Rorachu Watershed using Eq. 23.

Y_{IOE} = ((Elevation * 0.4617) + (Slope * 0.068) + (Aspect * 0.1722) +

(Geology * 0.2898) + (Soil * 0.4097) + (Drainage density * 0.0896) + (23)

(Road density * 0.2204) + (Rainfall * 0.3705) + (TWI * 0.0495) +

(SPI * 0.1303) + (TPI * 0.0041) + (NDVI * 0.1048) + (LULC * 0.532))

3.4 Multicollinearity test

Multicollinearity is a statistical testing phenomenon in which is tested the occurrences of intercorrelations among two or multiple independent variables with an earmarked degree of accuracy. Multicollinearity does not reduce the predictive power or reliability of the model as a whole; it only effects calculations regarding individual predictors (Fig. 9). previously using the landslide causative variables for the landslide susceptibility index (LSI) and landslide risk modeling, it is indispensable to test the multicollinearity of all the landslide causative factors (Zhou et al. 2018; Arabameri et al. 2019; Chen et al. 2018). Tolerance (TOL) and the Variance influencing factors (VIF) are both important indexes for multicollinearity diagnostic. VIF is just the reciprocal of tolerance (TOL). A tolerance (TOL) of less than 0.20 or 0.10 and/or a VIF of 5 or 10 and above implies a multicollinearity problem (O'Brien 2007). According to the Table 8, the smallest tolerance (TOL) of different models (BSI, IOE and WOE) were 0.321, 0.383 and 0.386 showing the rainfall parameter respectively. The variance influencing factors (VIF) of these models (BSI, IOE and WOE) are 3.115, 2.610 and 2.590 values showing rainfall parameter respectively. So there is no multicollinearity between independent landslide causative factors in this current research. The variance influencing factors (VIF) and the tolerance (TOL) as calculated following equations which is as follows

Table 8
Multicollinearity analysis of BSI, IOE and WOE approach

Factors	BSI		WOE		IOE	
	TOL	VIF	TOL	VIF	TOL	VIF
Elevation	0.634	1.577	0.589	1.697	0.524	1.908
Slope	0.568	1.760	0.598	1.672	0.592	1.688
Aspect	0.821	1.218	0.825	1.213	0.818	1.223
Geology	0.571	1.753	0.579	1.728	0.567	1.763
Soil	0.661	1.513	0.663	1.509	0.656	1.523
Drainage Density	0.559	1.789	0.772	1.296	0.552	1.811
Road density	0.847	1.181	0.845	1.183	0.844	1.185
TPI	0.705	1.418	0.626	1.598	0.621	1.611
TWI	0.686	1.459	0.527	1.898	0.524	1.910
SPI	0.863	1.158	0.715	1.399	0.714	1.400
NDVI	0.504	1.986	0.505	1.981	0.499	2.003
Rainfall	0.321	3.115	0.386	2.590	0.383	2.610
LULC	0.979	1.021	0.969	1.031	0.979	1.022

$$TOL = 1 - Ri^2$$

24

$$VIF = {}^{1}/_{1 - Ri^{2}}$$

25

TOL is the tolerance; VIF is the variance influencing factors and Ri^2 is the coefficient of determination of landslide conditioning factors *i*. The multicollinearity statistics of all the models (BSI, IOE and WOE) are shows in Table 8.

3.5 Models Validations/performances

The landslide susceptibility mapping was substantiated by different bivariate statistical (BSI, IOE and WOE) model in the Rorachu watershed. Without any proper validations of this statistical model performances are not compatible for landslide susceptibility analysis of any place in the world. The overall ascertainment of the landslide analysis is commonly justified on the total number of accurately classified pixels. In this study, the validation process was performed using total observed landslides (716 pixels) which were categorized into two i.e. i. 70% (500) landslides pixels were used for training the model and ii. Remaining 30% (216) landslides pixels were entrusted for the landslide validations. There are several approaches for the landslide susceptibility models validations. The validation can be made using *success rate curve* (Van westen et al. 2003; Chung and fabbri 1999) and *landslide density* (Gupta et al. 2008; Sarkar and Kanungo 2004), and *receiver operating characteristics* (ROC) curve. Here all the validations processes were employed for the compatible landslide susceptibility and landslide risk mapping in the Rorachu watershed.

3.6 Landslide risk mapping

The risk is the maximum prospective dimension of loss due to particular landslide events in a particular area and during certain time of period. Landslide hazard risk resolution aims to determine the probability of element-at-risk by the specific hazard will cause harm, and it inquire into the relevance between the instance of damaging events and the predominance of the consequences (Guzzetti et al. 2009). The risk analysis is very much significant for establishment of settlements in mountain areas, construction of roads, and land use practices. Varnes DJ. (1984), Fell (1994), Leroi (1996), and Xu et al. (2012) have successfully assessed landslide risk in different areas. According to the Xu et al. (2012), the risk is defined as the probability of damage caused by a particular hazard to a specific element is followed by this equation as

$$Risk = H \times V$$

26

Here, H denotes the Hazard expressed as probability of occurrence within a reference period and V define the Physical vulnerability of a particular type of element-at-risk (from 0 = not vulnerable and 1 = vulnerable) for a specific type of hazard and for a specific element-at-risk.

Result And Discussion

4.1 BSI model, landslide susceptibility zones and causative factors

The connection between landslide etiological factors and the location of the landslides has been performed by bivariate statistical index (BSI) model (Table 6). It is seen that 45^0 to 70^0 slope angles having maximum BSI (0.45) and of 0^0 to 15^0 slope class having lowest BSI with negative values of -0.91. On the other hand, the slope degree and slope instabilities are inversely related to each other in the Rorachu watershed. In the case of, the slope aspect, the SE, S and SW slope facets have been showing the positive BSI values (0.34, 0.28 and 0.76), and the NE, E, W and NW

slope facets have been showing the negative BSI values (-1.33, -0.001, − 0.02 and − 1.55). Flat and north facing slope aspect has no landslides. Among all these, the highest BSI values present in SW facing slope aspect. The BSI model values of altitude factor has been showing positive within the elevation range of 2516 to 3110 m, and 3110 to 4100 m elevation range exhibits the highest BSI value (BSI = 1.23).

The chungthang formation has the highest BSI value (BSI = 0.66) and the gorubathan formation has the lowest value (BSI = -2.67). The loamy skeletal, coarse loamy and coarse loamy holithic has the positive BSI values (1.28, 0.69 and 0.33, respectively) and the fine skeletal has the lowest BSI values (-3.88). The NDVI factor ranges between − 0.11 to 0.14 is represented highest BSI values (BSI = 0.82) which has been indicating the most favorable place for the landslide because of the diverse correlation between absence and presence of vegetation with slope instability. In the case of drainage density (DD), the highest BSI values (0.69) found in lowest drainage density areas. With regard to rainfall, the rainfall ranges from 1847 to 2386, 2386 to 2791 mm and 3096 mm/year having the highest landslides probability. On the other hand, the three classes of road density (RD) showed the strong favor of landslides. These classes are high (BSI = 0.86), moderate (BSI = 1.16) and low road density (BSI = 0.16). In the case of land use land cover (LULC), bare soil and open forest has the highest BSI values (1.40 and 0.29) representing a good correlation with the landslide. Similarly, the low SPI values represent the highest BSI values (0.26), the very low TPI values represent the highest BSI values (0.22) and the very low TWI values represent the strong correlation with landslide activities (Fig. 9).

4.2 Weight of evidence (WOE) model, landslide susceptibility zones and causative factors

The landslide susceptibility mapping (LSI) was made by using the weight of evidence (WOE) model (Fig. 10) using all variables class values (Table. 6). The WOE model is a bivariate statistical approach based on the Bayesian approach and it was first implemented for non-spatial and quantitative assessment in the medical sciences (Lusted 1968). The WOE bivariate statistical model allows us to calculate prior and posterior probability values and enumerate the weight contrast ($C = Wi^{+} - Wi^{-}$) of each class. The final landslide susceptibility index (LSI) value has been calculated combining all weight contrast (C) factors (Fig. 10). The altitude ranges between 3110 and 4100 m and 2516 and 3110 m represents the highest value of contrast weight of 1.50 and 1.22, respectively. The lowest elevation indicates the lowest weight. In the case of slope, the highest contrast (C) weight values (0.52 and 0.48) are found in the class of 45^0 to 70^0 and 35^0 to 45^0 which indicates the highest landslide probability. < 35^0 of slope angel showing the negative weight values which indicates the low landslide probability. The relationship between slope and weight contrast values are positively correlated. In the case of slope aspect, the south west (SW), Southeast (SE), South (S) directions and slopes were susceptible and very high risk for the landslide's occurrence with the highest values (C) of 0.95, 0.40 and 0.36, respectively, and all other slope aspect classes have been representing the negative values which indicates the lowest landslide probability. The low drainage density class showing the highest weight values (1.03). The high drainage density (DD) showing the negative weight values. In terms of geology, it is seen that chungthang formation and kanchenjunga formation represents positive weight values (0.90 and 0.52) and all other geological class exhibits the negative weight values that indicates the lowest probability of landslides. The loamy skeletal and coarse loamy soil classes having been significant probability of landslide susceptibility which showing the weight values of 1.42 and 1.01 respectively. The relationship between the rainfall and landslide occurrences have been showing that the rainfall class of 1847 to 2386 mm/year and 2386 to 2791 mm/year are characterized by the highest (C) probability of landslide occurrence. The moderate and high road density areas reveal the highest weight values of 1.48 and 0.95 respectively. In the Rorachu watershed the moderate RD class reveals the highest weight values that indicates the maximum landslide probability along the highway (NH 31A). For LULC, the highest landslide occurrence

probability observed in bare soil (1.59) and open forest (0.43). Other land use classes depict negative correlations between landslide occurrence probabilities and weight contrast values. The relationship between NDVI and landslide contrast weights are negatively correlated and vice versa. Very low NDVI class has the highest weight values (1.02). In case of SPI, the minimum values are associated with the highest weight value (0.38) and lower TWI values are accompanied by the highest contrast weight values (0.31). It has also been seen, that very low TPI classes have been representing the highest landslide probability (0.25) of occurrence.

4.3 Index of entropy (IOE) model, landslide susceptibility and causative factors

Figure 11. Landslide susceptibility map emanated by Index of Entropy (IOE) model

The landslide susceptibility index (LSI) was calculated by bivariate IOE model (Figure 11). In this model the every landslide causative factors classes has been represented by specific landslide probability instance density (Pij) and accordingly the final weight (Wij) was calculated. The landslide causative factors weight (Wij) and the probability densities (Pij) for every class of the landslide causative factors were derived to evaluate the landslide susceptibility (Table. 7). This bivariate IOE method allows us to calculate the weight for each landslide causative factors and the weighting process is based on the methodology which is proposed by Vlcko et al., (1980). The final landslide susceptibility index values have been derived using the IOE model (Figure 11). The calculated weights (Wij) of landslide causative factors indicates (Table 7). The most significant landslide causative factors are LULC (0.53), Elevation (0.46) and soil (0.41) (Fig. 12).

In terms of the landslide density (Pij), the altitude ranges between 3110 to 4100 m having the highest landslide density (Pij) values (0.52) and < 1500 m elevation areas have low landslide density (Pij) values (0.01). It is seen that the slope class of 45^0 to 70^0 is the highest probability of landslides where landslide density (Pij) value is 0.30. With regard to slope aspect, the south west, Southeast and South-facing and slopes were very high risk for the landslide's occurrence with the highest landslide density values (Pij) of 0.29, 0.19 and 0.18, respectively. The road density (RD) shows that moderate to high density areas has the highest landslide probability (Pij) values of 0.41 and 0.30, respectively. This situation is found at the places where one or two roads are very much effected by the landslides. It has been observed that the Chungthang formation and Kanchenjunga formation exhibits the highest probability of landslide density (Pij) values of 0.53 and 0.36, respectively (Fig. 12). Lingtse gnesis having no landslide density (Pij). With regard to soil, the highest landslide probability (Pij) was found in the class of loamy skeletal and coarse loamy where landslide density values (Pij) are 0.48 and 0.27, respectively. The rainfall class of 1847 to 2386 and 2386 to 2791 mm/year have been representing the highest (Pij) probability of landslide occurrence. In terms of drainage density (DD), it is seen that the low drainage density exhibits highest (pij) values of 0.40 and high drainage density exhibits low landslide probability (Pij) values of 0.09. The highest landslide probability (Pij) is observed in bare soil (0.64) and open forest (0.21). The moderate (0.30) and low (0.32) stream power index shows the highest probability of landslide density (Pij). The TWI and TPI also influence the landslide probability occurrence. The susceptibility of the landslide occurrences decreases with the increases of NDVI values and vice versa.

4.4 Result of model's validations

4.4.1 Landslide density (LD) method and model validations

Landslide density is the ratio among the observed landslides in that areas and the areas of every landslide susceptible classes (Table 9). The landslide density (LD) gradually increasing from the low landslide susceptible

class to high susceptible classes. It can be observed that the very high landslide susceptible classes have been representing the highest landslide density values of 0.0339 (BSI model), 0.0215 (IOE model) and 0.0331 (WOE model). Furthermore, there was a continuous decreases of landslide density values from the very high to low landslide susceptibility zones (Figure 13). BSI model and WOE model represents better result in comparison to IOE model.

Table 9
The comparisons between observed landslide and the landslide susceptibility zone with the landslide density (LD).

Model	Susceptibility Zones	No. of pixel	Area(Sq.km)	Area (%)	No. of landslide pixel	Area (Sq.km)	Area (%)	Landslide Density
BSI_M	Very low	14888	13.40	19.38	0	0	0	0
	Low	15340	13.81	19.97	8	0.01	1.12	0.0005
	Moderate	15782	14.20	20.55	49	0.04	6.84	0.0031
	High	15430	13.89	20.09	138	0.12	19.27	0.0089
	Very high	15366	13.83	20.01	521	0.47	72.77	0.0339
IOE_M	Very low	14883	13.39	19.38	24	0.02	3.35	0.0016
	Low	15943	14.35	20.76	91	0.08	12.71	0.0057
	Moderate	15005	13.50	19.54	101	0.09	14.11	0.0067
	High	16224	14.60	21.12	182	0.16	25.42	0.0112
	Very high	14751	13.28	19.21	318	0.29	44.41	0.0215
WOE_M	Very low	14741	13.27	19.19	0	0	0	0
	Low	15566	14.01	20.27	7	0.01	0.98	0.0004
	Moderate	15573	14.02	20.28	54	0.05	7.54	0.0035
	High	15352	13.82	19.19	139	0.13	19.41	0.0091
	Very high	15574	14.02	20.28	516	0.46	72.07	0.0331

(Bivariate Statistical Index Model (BSI_M), Index of Entropy Model (IOE_M) and Weight of Evidence Model (WOE_M))

4.4.2 Result of Success rate curve (SRC) method and model's validation

In this study area the cumulative percentage of observed landslides have been plotted against the cumulative percentage of landslide index (LSI) susceptibility zonation map to obtain the successive rate curve (SRC) against BSI, IOE and WOE (Fig. 14). The area under curve (AUC) was estimated for assessing the accuracy quantitatively. In this present study, the areas under curves (AUC) have been displaying the values of 0.869, 0.772 and 0.872, which means that the overall success rates are 86.9%, 77.20% and 87.20% for the bivariate statistical index (BSI), index of entropy (IOE) and weight of evidence (WOE) models respectively. This result has been indicating that the landslide susceptibility maps obtained by the bivariate statistical index (BSI) reflected more accuracy followed rather than index of entropy (IOE) and weight of evidence (WOE) models.

4.4.3 Result of Receive operating characteristics (ROC) curve method and model's validation

The validation of the landslide susceptibility maps can be made by receive operating characteristics (ROC) curve (Akgun et al. 2012; Regmi et al. 2014; Ozdemir and Altural 2013). A receipt operating characteristics (ROC) curve is a graphical plot which represent the diagnostic caliber of a binary classifier system as its discrimination threshold is varied. The ROC curve was created by plotting the true positive (TP) rate against the false positive (FP) rate at various threshold settings. The ROC curve is a proficient process for representing the quality of probability, deterministic detection and forecasting system. The area under curve (AUC) represents the quality of the landslide probabilistic models to feasible prediction of the occurrence and non-occurrence landslides. The accurate model has ascribe if the AUC values ranges between the 0.5 and 1, while the values below 0.5 represent the random fit and less reliable for the landslide susceptibility modelling (Yilmaz 2009a, b)

Sensitivity = TP / (TP + FN) (27)

Specificity = TN / (TN + FP) (28)

Specificity = 1 – Sensitivity (29)

In this study, the AUC values have been showing the various models are 0.858 (BSI model) and, we could say that the 85.80% prediction accuracy for this landslide susceptibility modelling in Rorachu watershed. The index of entropy (IOE) model presented 68.70% prediction accuracy and WOE model revealed 85.80% prediction accuracy of the landslide susceptibility mapping (Fig. 15) with the standard error of BSI (0.014), IOE (0.019) and WOE (0.014) models (Table 10). The BSI model and IOE models have been depicted the highest level of accuracy and may be accepted as significant statistical models for landslide susceptibility mapping.

Table 10
The overall statistics in the various models (Bivariate statistical index (BSI), Index of entropy (IOE) and Weight of evidence (WOE)).

Statistical Model	Area Under Curve (AUC)	Standard Error (SE)	Asymptotic Sig	Asymptotic 95% confidence interval	
				Lower Bound	Upper Bound
BSI_M	0.858	0.014	0.000	0.830	0.886
IOE_M	0.687	0.019	0.000	0.649	0.725
WOE_M	0.858	0.014	0.000	0.830	0.886

4.5 Analysis of landslide risk

The landslide risk (LR) map of the Rorachu watershed of Sikkim Himalaya (Fig. 16) has been made using geo-spatial tools. Firstly landslide susceptibility or hazard map was made using BSI, IOE and WOE models. The landslide vulnerability map was produced as vulnerability of settlement and road (vulnerability = 1 and non-vulnerability = 0). Finally, the landslide susceptibility and landslide vulnerability of which element-at-risk were combined (Eq. 26) to obtain the final landslide risk (LR) map of the Rorachu Watershed. The landslide risk (LR) map has been classified into five categories i.e. very low, low, moderate, high and very high (Fig. 16). The prepared landslide risk map has been revealed that 20.01% (0.67 km^2), 20.39% (0.68 km^2) and 19.29% (0.64km^2) (Table 12) of the settlement areas

occupied very high (VH) risk areas as obtained by BSI, IOE and WOE statistical model, respectively. The 19.01% (0.64 km^2), 19.07% (0.65km^2) and 17.77% (0.60 km^2) (Table 11) of the road areas are under very high (VH) risk as obtained by BSI, IOE and WOE models respectively. It has been observed that, the most of the settlements and roads have been built up on very high risk area which is observed in the eastern part of the Rorachu watershed.

Table 12
Areal distribution of BSI, IOE and WOE approach based landslide Risk assessment (LRA) mapping of Settlement

Landslide Risk (LR) zones	BSI		IOE		WOE	
	Area (km^2)	Area (%)	Area (km^2)	Area (%)	Area (km^2)	Area (%)
Very Low (VL)	0.6543	19.45	0.6543	19.45	0.6714	19.96
Low (L)	0.6849	20.36	0.6723	19.99	0.6561	19.51
Moderate (M)	0.6669	19.83	0.6804	20.23	0.7065	21.01
High (H)	0.6831	20.31	0.6705	19.94	0.6804	20.23
Very High (VH)	0.6741	20.04	0.6858	20.39	0.6489	19.29

4.6 Triggering factors

Landslides may be a consequence of several geomorphic, climatic, litho-tectonic and anthropogenic factors. But the fact is that, which factors obtain leading role for the instance of landslides in any place in the world even in Rorachu watershed. There are several researchers to employ the landslide susceptibility mapping in distinct part of the world. Many researchers are excellent, recite to which factors, are more effective for landslide susceptibility mapping or slope instability mapping (Pradhan and Kim, 2014; Lee and Min 2001; Melchiorre et al. 2008). Slope degree remains an extremely relevant parameter in the slope instability analysis, and it is repeatedly exploit for the preparing of landslide susceptibility maps (Lee and Min 2001; Saha et al. 2005; Gorsevski et al. 2012).

Altitude has also frequently conditioning factor for landslide susceptibility analysis because it is permitted by various geological and geomorphological processes (Gorsevski et al. 2012; Pourghasemi et al. 2012b; Pradhan and Kim 2014). Earthquake and rainfall also a critical factor for landslides susceptibility mapping. In this study, for the mapping of the landslide susceptibility and landslide risk (LR), we exercise thirteen landslide causative factors. The elite opinion and experimental knowledge employed to consider Altitude, Slope, Aspect, and Rainfall (Fig. 17) as triggering factors for the landslides susceptibility index (LSI) mapping and Landslide risk (LR) mapping of the Rorachu Watershed. In this study area the ultimate probability of landslide vulnerabilities and encumbrance of landslides is related with lofty altitude, rainfall and slope. In Rorachu watershed, the altitude (2500–4,110 m), slope (35^0 – 70^0) and rainfall (2300–3000 mm) have excessive affect for the landslides.

The direct impact of monsoonal rainfall on landslides in this Rorachu watershed. In this landslide risk assessment study, we are trying the correlating among the triggering factors and landslide susceptibility models (BSI, IOE and WOE). The relationship among the altitude and landslide susceptibility models (BSI, IOE and WOE) has been showing the altitude between 2500 and 4000 meters has the absolute concentration of landslide probability (Fig. 17).Accordingly, the relations between the slope and landslides susceptibility model (BSI, IOE and WOE) are also showing the slope between 25^0 and 45^0 highest concentrations of landslide probability. And also seen the relationship between rainfall and bivariate statistical models (BSI, IOE and WOE) between 2000–2500 mm and

3200–3500 mm represent the highest concentration of landslides probability (Fig. 15). In the matter of aspect, it has seen the South west (SW), South east (SE) and south facing slope aspect have been indicating the significant vulnerability of landslides by the BSI, IOE and WOE statistical models.

Conclusion

The Himalayan mountain ranges have been showing one of the most disastrous areas in this world. Landslide is one of them in which is most significant natural hazard in this region. Since landslides are a significant threat to the damage of lives and properties due to its hazardous character in this Sikkim Himalaya. Various methodological processes have been obtained for the landslide susceptibility modelling (LSM) and landslide risk (LR) mapping around the world. The current study has been addressing this issues exercising the bivariate statistical index (BSI), index of entropy (IOE) and weight of evidence (WOE) approaches in Rorachu watershed of East Sikkim, India. This study is first time apply for the identification of landslide risk areas (LRA) in NH31A roads and also apply for the population vulnerability. The validation has been made by using ROC, LD and SRC methods in which the accuracy of the Landslide risk (LR) and landslide susceptibility index (LSI) map emanated by BSI, IOE and WOE models. The study revealed that the bivariate statistical model experienced with reasonably good accuracy for the landslide susceptibility and landslide risk (LR) mapping of the Rorachu watershed. The triggering factors have major role for the landslide activities in this area. In this study area, NH 31A road is more vulnerable (more than 19% areas at high risk) to landslide and landslide risk (LR) zonation map also indicates the highest vulnerability. More than 20% settlement areas have been showing Very high (VH) landslide risk. The landslide susceptibility zonation map revels that the 27% areas remain very high to high landslide susceptibility zone as of BSI model, 27.80% areas remain very high to high landslide susceptibility zone as of IOE model and 40.25% areas remain very high to high landslide susceptibility zone as of WOE model. In summary, the results of the study suggests that the landslide susceptibility index (LSI) and landslide risk (LR) mapping techniques can be used for mitigating hazard associated with the landslides in the Rorachu watershed. We are suggesting for the further work that it would be better if the identification of landslide risk areas to major roads and settlements in the whole Sikkim state. This susceptibility and landslide risk (LR) map of Rorachu watershed can be used in future for slope management, land use planning, urban planning, disaster management planning and road construction, etc.

Declarations

Conflicts of interest

The authors declare that they have no known competing financial interests or personal relationships that could have appeared to influence the work reported in this paper.

Availability of data: Data available on request from the authors

Template for data availability: The data that support the findings of this study are available from the corresponding author, [author initials], upon reasonable request.

Statement policy: Basic, Share upon Request

Author contribution

Sk Asraful Alam: Methodology, Formal analysis, Investigation, Writing - Original draft. **Ramkrishna Maiti:** Methodology, Investigation, Writing - review & editing. **Sujit Mandal:** Methodology, Investigation, Writing - review & editing.

Author's details

1. Mr. Sk Asraful Alam[1*]

2. Dr. Ramkrishna Maiti[1]

3. Dr. Sujit Mandal[2]

[1]Research Scholar, Department of Earth System Science (ESS), Vidyasagar University, Midnapore, Email – alamrsgis13@gmail.com

[1]Professor and Head, Dept. of Geography & Environment Management, Vidyasagar University, Midnapore, Email - ramkrishna@mail.vidyasagar.ac.in

[2]Professor, Dept. of Geography, Diamond Harbour Women's University, West Bengal-743368

Email- mandalsujit2009@gmail.com

- Corresponding author.

E-mail address: alamrsgis13@gmail.com (Sk Asraful Alam)

ORCID - https://orcid.org/0000-0002-9501-9198

References

1. Arabameri A, Pradhan B, Rezaei K, Sohrabi M, & Kalantari Z, (2019) GIS-based landslide susceptibility mapping using numerical risk factor bivariate model and its ensemble with linear multivariate regression and boosted regression tree algorithms. J Mt Sci, 16(3), 595–618.
2. Akgun A, Needet T, (2010) Landslide susceptibility mapping for Ayvalik (Western Turkey) and its vicinity by multi criteria decision analysis. Environ. Earth Sci. 61, 595–611.
3. Akgun A, Serhat D, Fikri B, (2008) Landslide susceptibility mapping for a landslide-prone area (Findikli, NE of Turkey) by likelihood-frequency ratio and weighted linear combination models. Environ Geol 54, 1127–1143.
4. Akgun A, Sezer EA, Nefeslioglu HA, Gokceoglu C, Pradhan B, (2012) An easy-touse MATLAB program (MamLand) for the assessment of landslide susceptibility using a Mamdani fuzzy algorithm. Computers & Geosciences 38 (1), 23–34.
5. Aleotti P, Chowdhury R, (1999) Landslide hazard assessment: summary review and new perspectives. Bull Eng Geol Environ 58:21–44
6. Ayalew, L., Yamagishi, H., Maruib, H., Takami, K., 2005. Landslide in Sado Island of japan: part II. GIS-based susceptibility mapping with comparisons of results from two methods and verifications. Eng Geol 81(4):432–445
7. Ayalew, L., Yamagishi, H., 2005. The application of GIS-based logistic regression for landslide susceptibility mapping in the Kakuda Yahiko Mountains, Central Japan. Geomorphology 65:15–31
8. Bednarik, M., Magulova B., Matys, M., Marschalko, M., 2010. Landslide susceptibility assessment of the Kralovany–Liptovsky Mikulas railway case study. Phys Chem Earth 35, 162–171.

9. Bednarik, M., Yilmaz, I., Marschalko, M., 2012. Landslide hazard and risk assessment: a case study from the Hlohovec-Sered landslide area in southwest Slovakia. Nat Hazards. http://dx.doi.org/10.1007/s11069-012-0257-7.
10. Beven, KJ., Kirkby, MJ., 1979. A physically based, variable contributing area model of basin hydrology. Hydro Sci Bull 24:43–69
11. Bonham-Carter, G. F., Agterberg, F. P., & Wright, D., F. 1988. Integration of geological datasets for gold exploration in Nova Scotia. PE & RS, 54, 1585–1592.
12. Cevik, E., Topal, T., 2003. GIS-based landslide susceptibility mapping for a problematic segment of the natural gas pipeline, Hendek (Turkey). Environ Geol 44:949–962
13. Chen, W., Shahabi, H., Shirzadi, A., Hong, H., Akgun, A., Tian, Y., Liu, J., Zhu, A., & Li, S., 2018. Novel hybrid artificial intelligence approach of bivariate statistical-methods-based kernel logistic regression classifier for landslide susceptibility modeling, Bull Eng Geol Environ. (2019) 78:4397–4419 https://doi.org/10.1007/s10064-018-1401-8
14. Chung, CF., Fabbri, AG, van Westen, CJ., 1995. Multivariate regression analysis for landslide hazard zonation. In: Carrera A, Guzzetti F (eds) Geographical information systems in assessing natural hazards. KAP, Dordrecht, pp 107–133
15. Chung, CF., and Fabbri, AG., 1993. The representation of geosciences information for data integration; Non-renewable Resour. **2(2)** 122–139.
16. Constantin, M., Bednarik, M., Jurchescu, M. C., and Vlaicu, M., 2011. Landslide susceptibility assessment using the bivariate statistical analysis and the index of entropy in the Sibiciu Basin (Romania); Environ. Earth Sci. **63(2)** 397–406.
17. Dahal, R. K., Hasegawa, S., Nonomura, A., Yamanaka, M., Dhakal, S., & Paudyal, P., 2008a. Predictive modeling of rainfall-induced landslide hazard in the lesser Himalaya of Nepal based on weights-of-evidence. Geomorphology, 102(3), 496–510.
18. Dahal, R. K., Hasegawa, S., Nonomura, A., et al., 2008b. GIS-Based Weights-of-Evidence Modelling of Rainfall-Induced Landslides in Small Catchments for Landslide Susceptibility Mapping. Environ Geol, 54(2): 311–324, doi: 10.1007/s00254-007-0818-3
19. Dai, F., Lee, C., Li, J., and Xu, Z., 2001. Assesment of landslides susceptibility on the natural terrain of lantau Island, Hong Kong. Environ Geol, 40, 381–391.
20. Devkota, K., Regmi A.D., Pourghasemi, H.R., Yishida, K., Pradhan, B., Ryu, I.C., Dhital, M.R., althuwaynee, O.F., 2012. Landslide susceptibility mapping using certainty factor. Index of entropy and logistic regression models in GIS and their comparision at Mugling – Narayanghat road section in Nepal Himalaya. Nat Hazards.
21. Devkota, K. C., Regmi, A. D., Pourghasemi, H. R., Yoshida, K., Pradhan, B., Ryu, I. C., Dhital, M. R., and Althuwaynee, O. F., 2013, Landslide susceptibility mapping using certainty factor, index of entropy and logistic regression models in GIS and their comparison at Mugling–Narayanghat road section in Nepal Himalaya; Nat. Hazards **65** 135–165.
22. Ercanoglu, M., Gokceoglu, C., 2002. Assessment of landslide susceptibility for a landslide prone area (north of Yenice, NW Turkey) by fuzzy approach. Environ Geol 41:720–730
23. Fell, R., 1994. Landslide risk assessment and acceptable risk. Can Geotech J 31:261– 272
24. Guisan, A., Weiss, S.B., Weiss, A.D., 1999 GLM versus CCa spatial modeling of plant species distribution. Plant Ecol 143: 107–122.

25. Gupta, R.P., Kanunga, D.P., Arora, M.K., and Sarkar S., 2008. Approaches for comparative evolution of raster GIS-based landslide susceptibility zonation maps. Int Jour Appld Earth Obs geoinf, v.10, pp.330–341.
26. Guzzetti, F., Carrara, A., Cardinali, M., Reichenbach, P., 1999. Landslide hazard evaluation: a review of current techniques and their application in a multi-scale study, Central Italy. Geomorphology 31:181– 216
27. Guzzetti, F., Reichenbach, P., Ardizzone, F., Cardinali, M., & Galli, M., 2009. Landslide hazard assessment, vulnerability estimation and risk evaluation. An example from the Collazzone Area (Central Umbria, Italy). Geogr Fis Dinam Qual, 32, 183–192.
28. Gokceolu, C., Sonmez, H., Nefeslioglu, HA., Duman, T.Y., Can, T., 2005. The 17 March 2005 Kuzulu landslide (Sivas, Turkey) and landslide-susceptibility map of its near vicinity. Eng Geol 81:65–83
29. Gorsevski, P. V., Donevska, K. R., Mitrovski, C. D., and Frizado, J. P., 2012. Integrating multi-criteria evaluation techniques with geographic information systems for landfill site selection: A case study using ordered weighted average; J Waste Manag 32(2) 287–296.
30. Hengl, T., Gruber, S., Shrestha, D.P., 2003. Digital terrain analysis in ILWIS. International Institute for Geo-Information Science and Earth Observation Enschede, The Netherlands, p 62
31. Horton, R.E., 1932. Drainage basin characteristics. Trans. Am. Geophys. Union 13, 350–361.
32. Horton, R.E., 1945. Erosional development of streams and their drainage basins: a hydro physical approach to quantitative morphology. Geol. Soc. Am. Bullet. 56, 275–370.
33. Jaafari, A., Najafi, A., Pourghasemi, H. R., Rezaeian, J., and Sattarian, A., 2014. GIS-based frequency ratio and index of entropy models for landslide susceptibility assessment in the Caspian forest, northern Iran; Int. J. Environ. Sci. Tech. **11(4)** 909–926.
34. Lee, S., Choi, J., 2004. Landslide Susceptibility Mapping Using GIS and the Weight-of-Evidence Model. Int J Geogr Inf Sci, 18(8): 789–814, doi:10.1080/13658810410001702003
35. Lee, S., Min, K., 2001. Statistical analysis of landslide susceptibility at Yongin, Korea. Environ. Geol. 40, 1095–1113.
36. Lee, S., Choi, J., Chwae, U., & Chang, B., 2002a. Landslide susceptibility assessment using weight of evidence. Geosci Remote Sens Symp, IEEE, 5, 2865–2867.
37. Lee, E.M., Zones, D.K.C., 2004. Landslide Risk Assessment. Thomas Telford, London
38. Leroi, E., 1996. Landslide hazard—risk maps at different scales: objectives, tools and development. In: Senneset K (eds) Landslides—Glissements de Terrain, 7th International symposium on landslides. Balkema, Trondheim, Norway, pp 35–51
39. Li, X.J., Chen, Y.N., Ouyang, H., 2002. Analysis on sand disaster with disaster entropy method. Arid Land Geography 25 (4), 350–353.
40. Lusted, L.B., 1968. Introduction to medical decision making. Charles C. Thomas, Springfield III. 271.
41. Ma, S., Qiu, H., Hu, S., Pei, Y., Yang, W., Yang, D., & Cao, M., 2019. Quantitative assessment of landslide susceptibility on the Loess Plateau in China. Phys Geog, 1–28.
42. Mandal, S., Mandal, K., 2017a. Bivariate statistical index for landslide susceptibility mapping in the Rorachu river basin of eastern Sikkim Himalaya, India. Spat Inf Res 26(1):59–75
43. Marcini, F., Ceppi, C., & Ritrovato, G., 2010. GIS and statistical analysis for landslide susceptibility mapping in the Daunia area, Italy. Nat Haz Earth Sys Sci, 10, 1851–1864. https://doi.org/10.5194/nhess-10-1851-2010.
44. Mathew, J., Jha, V. K., & Rawat, G., 2007. Weights of evidence modeling for landslide hazard zonation mapping in part of Bhagirathi valley, Uttarakhand. Curr Sci, 92(5), 628.

45. Melchiorre, C., Matteucci, M., Azzoni, A., Zanchi, A., 2008. Artificial neural networks and cluster analysis in landslide susceptibility zonation. Geomorphology 94:379–400
46. Moore, I.D., Grayson, R.B., Ladson, A.R., 1991. Digital terrain modelling-a review of hydro-hydrological, geomorphological, and biological application. Hydrol. Process 5, 3–30.
47. Mon, D.L., Cheng, C.H., Lin, J.C., 1994. Evaluating weapon system using fuzzy analytic hierarchy process based on entropy weight. Fuzzy Sets and Systems 62 (2), 127–134.
48. Naithani, A.K., 1999. The Himalayan landslides. Employment News 23(47):20–26
49. O'Brien, R.M., 2007. A caution regarding rules of thumb for variance inflation factors. Qual Quant 41(5):673–690
50. Oh, H. J., Lee, S., 2011. Landslide Susceptibility Mapping on Panaon Island, Philippines Using a Geographic Information System. Environ Earth Sci, 62(5): 935–951, doi:10.1007/s12665-010-0579-2
51. Ozdemir, A., Altural, T., 2013. A comparative study of frequency ratio, weights of evidence and logistic regression methods for landslide susceptibility mapping: Sultan Mountains, SW Turkey. J Asian Earth Sci 64:180–197
52. Pourghasemi, H.R., 2008. Landslide hazard assessment using fuzzy logic (case study: a part of Haraz Watershed). M.Sc Thesis, Tarbiat Modarres University International Campus, Iran, 92 p.
53. Poudyal, C.P., Chang, C,Oh, HJ., Lee, S., 2010. Landslide susceptibility maps comparing frequency ratio and artificial neural networks: a case study from the Nepal Himalaya. Environ Earth Sci 61:1049–1064
54. Pradhan, B., Youssef, A.M., 2010. Manifestation of remote sensing data and GIS on landslide hazard analysis using spatial-based statistical models. Arab J Geosci 3 (3), 319–326.
55. Pradhan, B., Mansor, S., Pirasteh, S., Buchroithner, M., 2011. Landslide hazard and risk analyses at a landslide prone catchment area using statistical based geospatial model. Int J Remote Sens 32 (14), 4075–4087. http://dx.doi.org/10.1080/01431161.2010.484433.
56. Pradhan, B., Chaudhari, A., Adinarayana, J., Buchroithner, M.F., 2012. Soil erosion assessment and its correlation with landslide events using remote sensing data and GIS: a case study at Penang Island, Malaysia. Environ Monit Asses 184 (2), 715–727.
57. Pradhan, B., Lee, S., 2010a. Delineation of landslide hazard areas on Penang Island, Malaysia, by using frequency ratio, logistic regression, and artificial neural network models. Environ Earth Sci 60(5): 1037–1054
58. Pradhan, A. M.S., and Kim, Y. T., 2014. Relative effect method of landslide susceptibility zonation in weathered granite soil: A case study in Deokjeok-ri Creek, South Korea; Nat. Hazards 72(2) 1189–1217.
59. Pourghasemi, H.R., Pradhan, B., Gokceoglu, C., Mohammadi, M., Moradi, H.R., 2013b. Application of weights-of-evidence and certainty factor models and their comparison in landslide susceptibilitymapping at Haraz watershed. Iran Arab J Geosci 6:2351–2365
60. Pourghasemi, H. R., Pradhan, B., Gokceoglu, C., and Moezzi, K. D., 2012b. Landslide susceptibility mapping using a spatial multi criteria evaluation model at Haraz Watershed, Iran; In: Terrigenous Mass Movements, Springer-Berlin Heidelberg, pp. 23–49.
61. Rautela, P., Lakhera, R.C., 2000. Landslide risk analysis between Giri and Tons Rivers in Himachal Himalaya (India). Int J Appl Earth Obs Geoinf 2:153–160
62. Rawat, M.S., and Joshi, V., 2016. Landslide hazard zonation in Rorachu sub watershed of east district of Sikkim, India, conference paper.
63. Regmi, A.D., Yoshida, K., Pradhan, B., Pourghasemi, H.R., Khumamoto, T., Akgun, A., 2014. Application of frequency ratio, statistical index and weights-of-evidence models, and their comparison in landslide susceptibility mapping in Central Nepal Himalaya. Arab J Geosci. doi:10.1007/s12517-012-0807-z

64. Regmi, N. R., Giardino, J. R., & Vitek, J. D., 2010. Modeling susceptibility to landslides using the weight of evidence approach: Western Colorado, USA. Geomorphology, 115(1), 172–187.
65. Regmi, N.R., Giardino, J.R., and Vitek, J.D., 2010a. Assessing susceptibility to landslide: Using models to understand observed changes in slopes. Geomorphology, 122, 25–38.
66. Ren, L.C., 2000. Disaster entropy: conception and application. J Nat Disaster 9 (2), 26–31.
67. Saha, A.K. et al., 2005. An approach for GIS based statistical landslide susceptibility zonation with a case study in the Himalayas. Landslides 2, 61–69.
68. Sahabi, H., Hhezri, S., Ahmha, B.B., and Hashim, M., 2014. Landslide susceptibility mapping at central Zab basin, Iran: A comparision between analytical hierarchy process, Frequency ratio and logistic regression models. Catena, 115, 55–70
69. Sarkar, S., and Kanungo, D.P., 2004. An integrated approach for landslides susceptibility mapping using remote sensing and GIS. PE & RS, v.70(5), pp.617–625.
70. Shannon, C.E., 1948. A mathematical theory of communication. Bull Syst Technol J 27(3):379–423
71. Singh, L. P., van Westen, C. J., Champati Ray, P. K., et al., 2005. Accuracy Assessment of InSAR Derived Input Maps for Landslide Susceptibility Analysis: A Case Study from the Swiss Alps. Landslides, 2(3): 221–228, doi:10.1007/s10346-005-0059-z
72. Soeters, R., van Westen, C.J., 1996. Slope instability recognition analysis and zonation. In: Turner KT, Schuster RL (eds) Landslides: investigation and mitigation. Special Report No. 247, pp 129–177, Transportation Research Board National Research Council, Washington, DC.
73. Strahler, A.N., 1952. Hypsometric (area-altitude) analysis of erosional topography. Geol. Soc. Am. Bullet. 63, 117–142.
74. van Westen, C.J., Rengers, N., Terlien, M.T.J., Soeters, R., 1997. Prediction of the occurrence of slope instability phenomena through GIS based hazard zonation. Geol Rundsch 86:404–414
75. Van Western, C.J., 2002. Use of Weights of Evidence Modeling for Landslide Susceptibility Mapping, 21 pp.
76. Van Westen, C.J., Rengers, N. and Soeters, R., 2003. Use of geomorphological information in indirect landslides susceptibility assessment, Nat Hazards, v.30, pp.399–419.
77. Varnes, D.J., 1984. Landslide hazard zonation: a review of principles and practice. United Nations International, Paris
78. Wan, S., 2009. A spatial decision support system for extracting the core factors and thresholds for landslide susceptibility map. Eng Geol 108, 237–251.
79. Wan, S., Lei, T.C., 2009. A knowledge-based decision support system to analyze the debris-flow problems at Chen-Yu-Lan River, Taiwan. Knowl Based Syst 2 (8), 580–588.
80. Youssef, A. M., Al-Kathery, M., and Pradhan, B., 2014a. Landslide susceptibility mapping at Al-Hasher area, Jizan (Saudi Arabia) using GIS-based frequency ratio and index of entropy models; Geosci. J. **19(1)** 113–134.
81. Wu, Z., Wu, Y., Yang, Y., Chen, F., Zhang, N., Ke, Y., et al., 2017. A comparative study on the landslide susceptibility mapping using logistic regression and statistical index models. Arab J Geosci, 10, 187. https://doi.org/10.1007/s12517-017-2961-9.
82. Xu, C., F. Dai, X. Xu, and Y. H. Lee., 2012. “GIS-based Support Vector Machine Modeling of Earthquake-Triggered Landslide Susceptibility in the Jianjiang River Watershed, China.” Geomorphology 145: 70–80. doi:10.1016/j.geomorphology.2011.12.040.

83. Yalcin, A., 2008. GIS-based landslide susceptibility mapping using analytical hierarchy process and bivariate statistics in Ardesen (Turkey): comparisons of results and confirmations. Catena 72, 1–12.
84. Yang, Z., Qiao, J., 2009. Entropy-based hazard degree assessment for typical landslides in the Three Gorges Area, China. In: Wang F, Li T (eds) Landslide disaster mitigation in Three Gorges Reservoir, China. Environ Sci Engin. Springer, Berlin, pp 519–529
85. Yilmaz, I., 2009a. A case study from Koyulhisar (Sivas-Turkey) for landslide susceptibility mapping by artificial neural networks. B Eng Geol Environ 68:297–306
86. Yilmaz, I., 2009b. Landslide susceptibility mapping using frequency ratio, logistic regression, artificial neural networks and their comparison: a case study from Kat landslides (Tokat-Turkey). Comput Geosci 35:1125–1138
87. Yufeng, S., Fengxiang, J., 2009. Landslide stability analysis based on generalized information entropy. In: 2009 international conference on environmental science and information application technology, pp 83–85
88. Yi, C.X., Shi, P.J., 1994. Entropy production and natural hazard. J Bej Normal Univ (Natural Science Edition) 30 (2), 276–280.
89. Youssef, A. M., Al-Kathery, M., and Pradhan, B., 2014a. Landslide susceptibility mapping at Al-Hasher area, Jizan (Saudi Arabia) using GIS-based frequency ratio and index of entropy models; Geosci. J. **19(1)** 113–134.
90. Youssef, A. M., Pradhan, B., Jebur, M. N., and El-Harbi, H. M., 2014b. Landslide susceptibility mapping using ensemble bivariate and multivariate statistical models in Fayfa area, Saudi Arabia; Environ. Earth Sci. **73(7)** 3745– 3761.
91. Zhou, C., Yin, K., Cao, Y., Ahmed, B., Li, Y., Catani, F., & Pourghasemi, H. R., 2018. Landslide susceptibility modeling applying machine learning methods: A case study from Longju in the Three Gorges Reservoir area, China. Computers & geosciences, 112, 23–37.

Tables

Tables 11 is not available with this version.

Figures

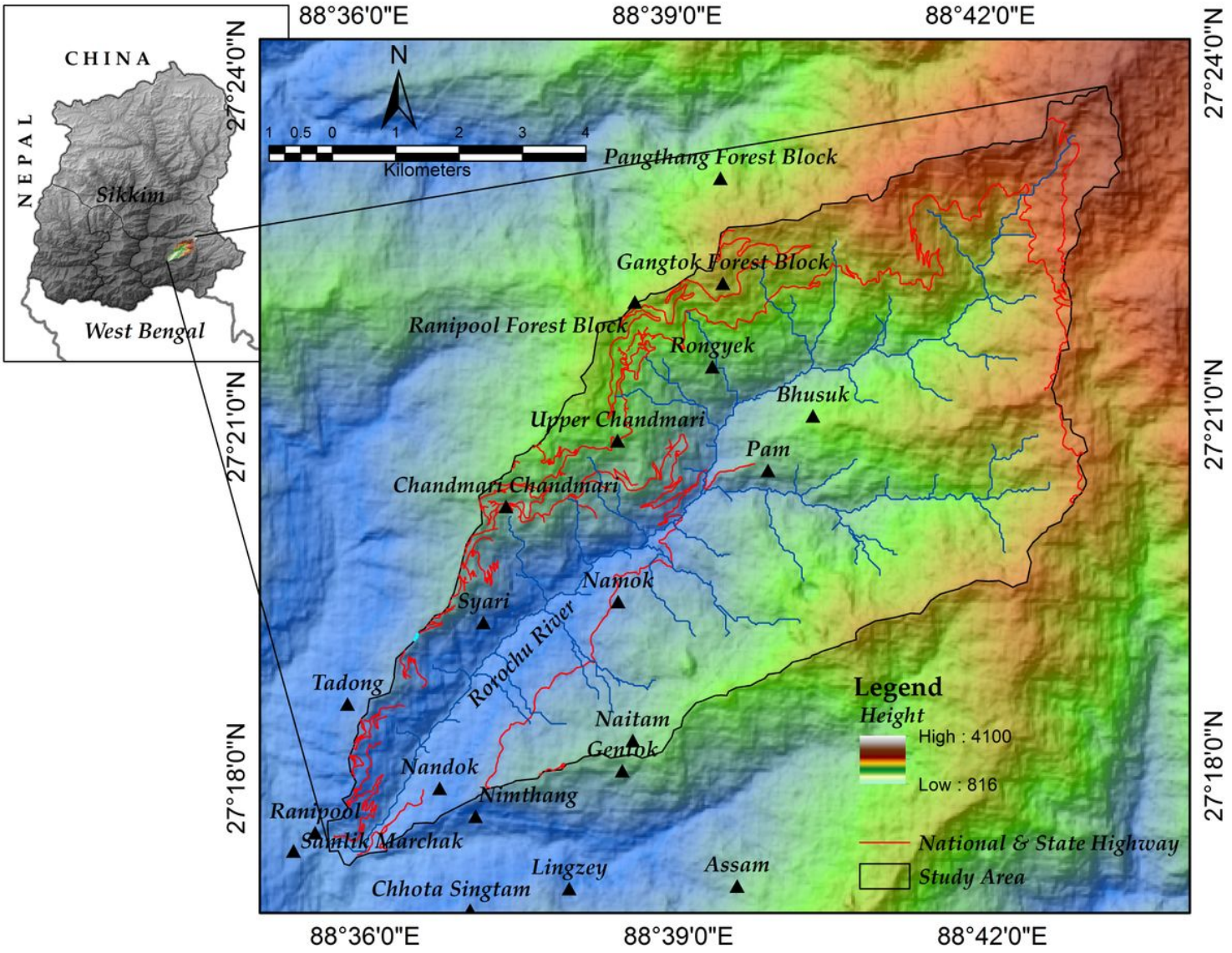

Figure 1

Location map of the study area

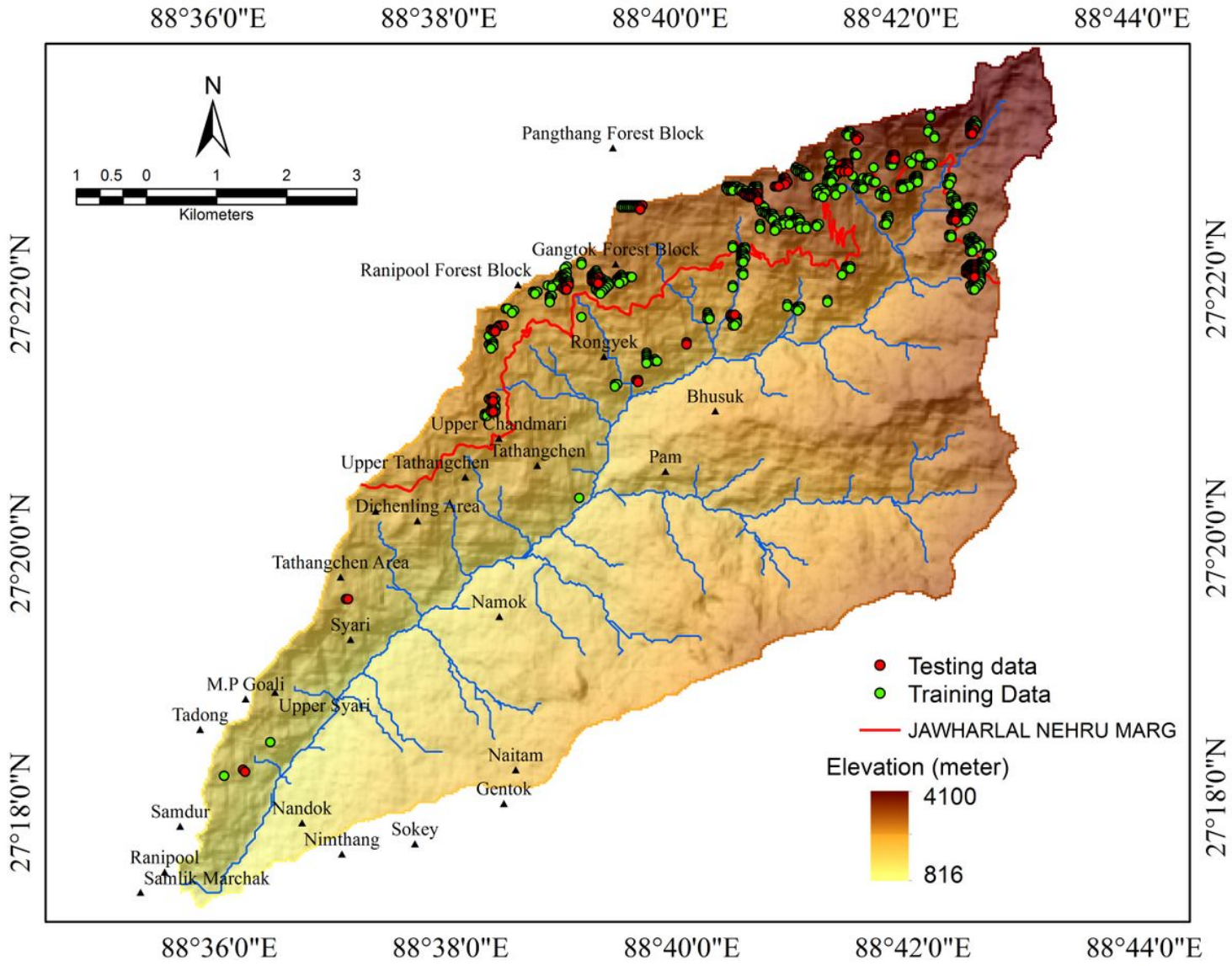

Figure 2

Landslide inventory map of Rorachu watershed

Image not available with this version

Figure 3

Methodological flow chart

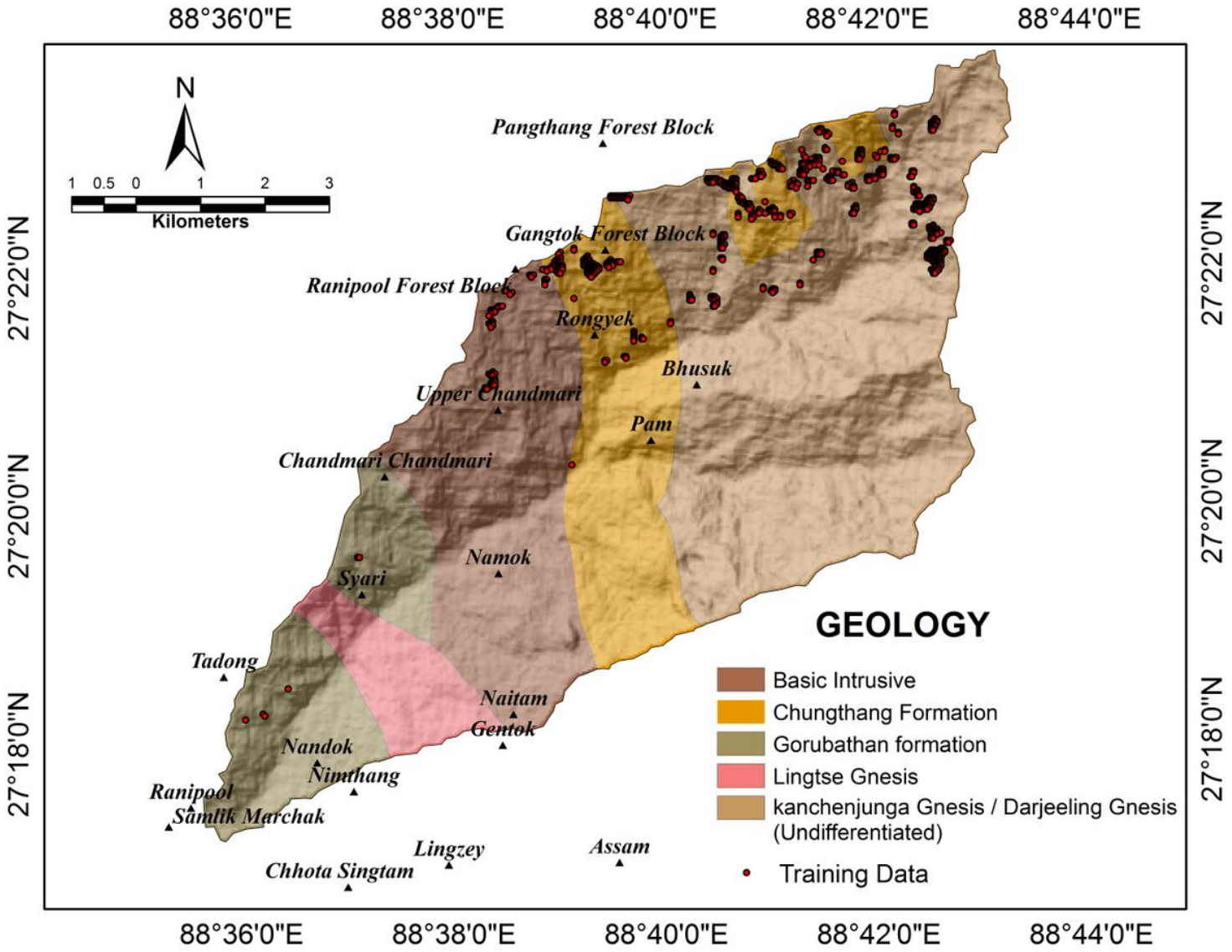

Figure 4

Geological map of the study area

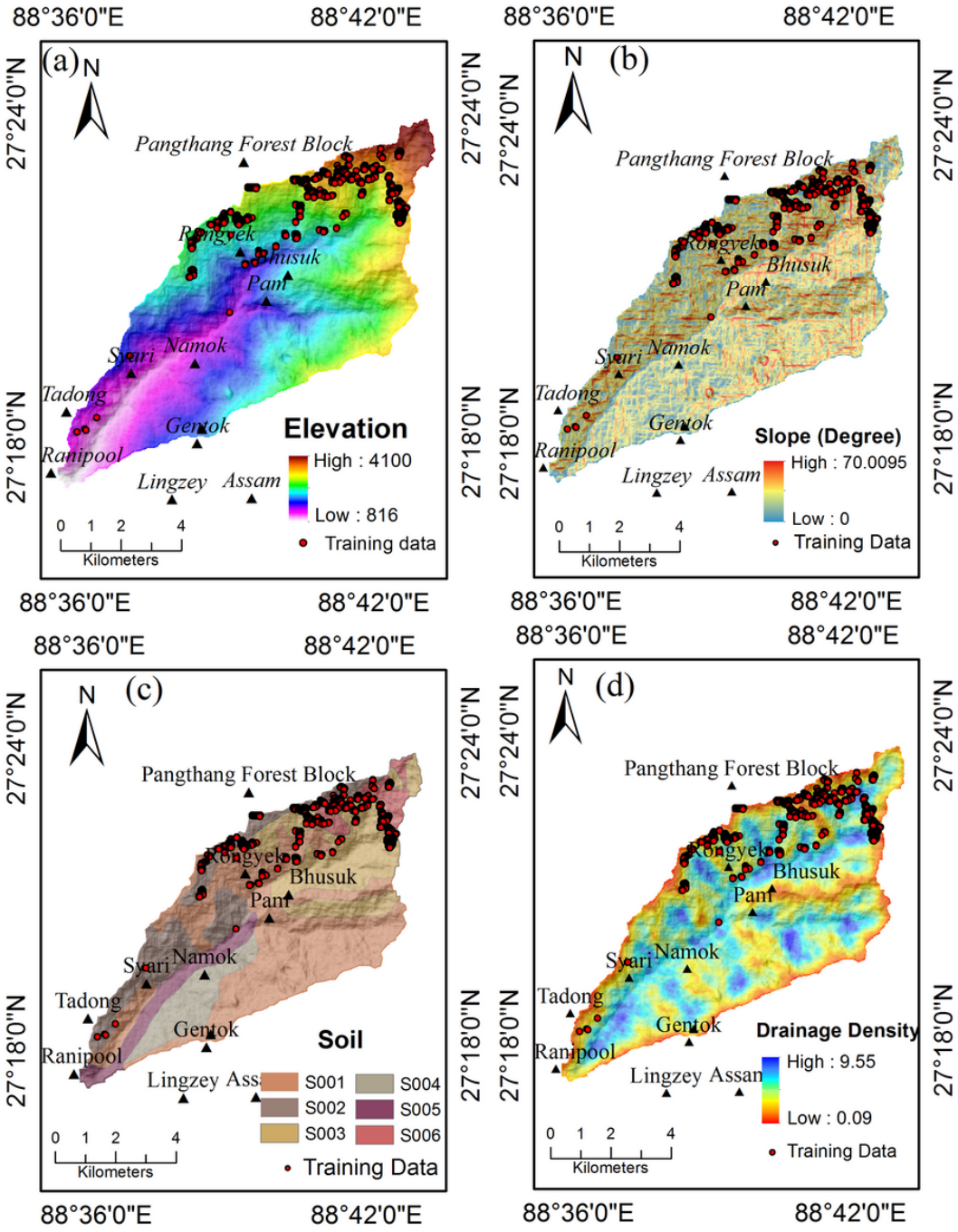

Figure 5

Landslide conditioning factors a. Elevation b. Slope c. Soil d. Drainage density

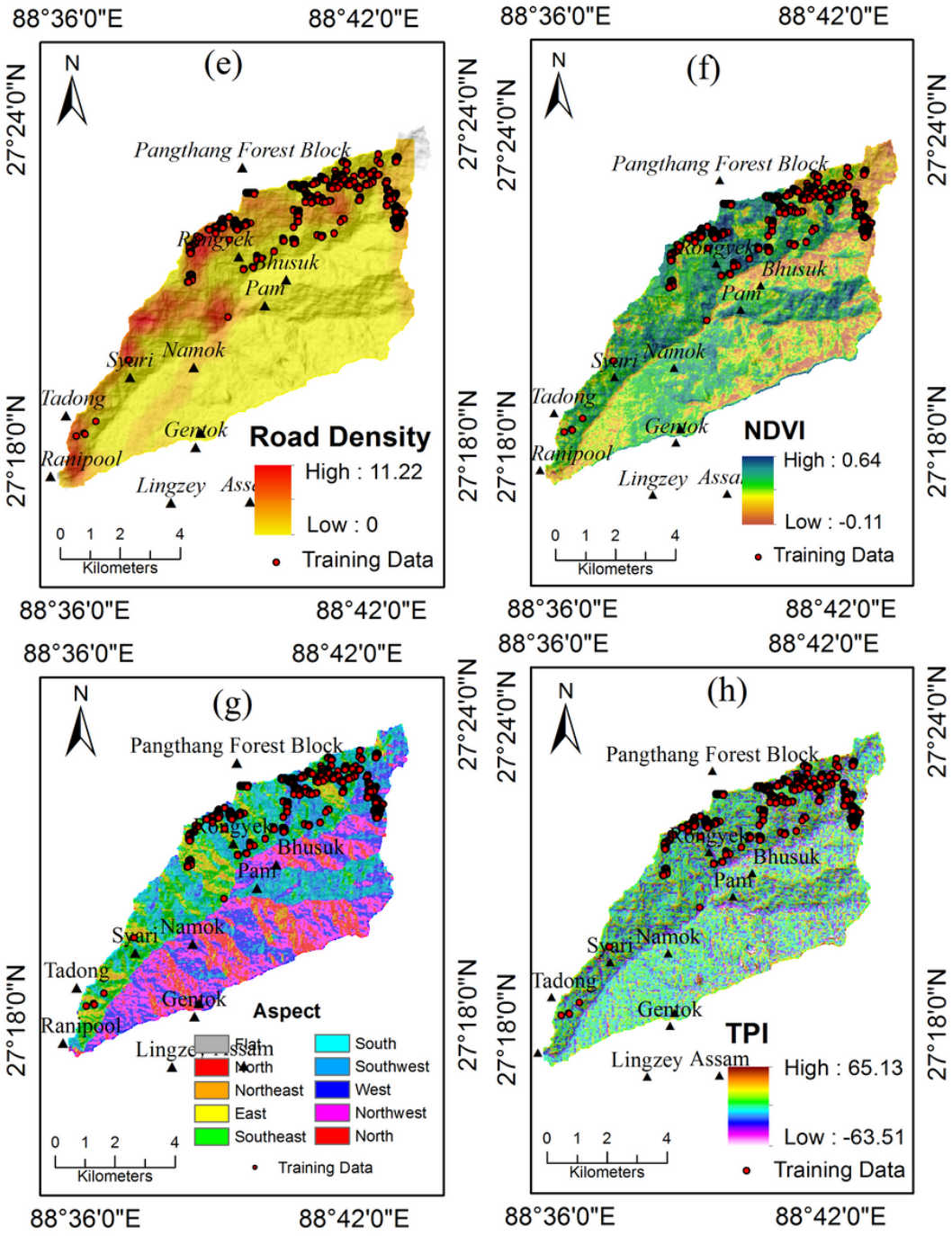

Figure 6

Landslide conditioning factors e. Road density f. NDVI g. Aspect

h. Topographic position index (TPI)

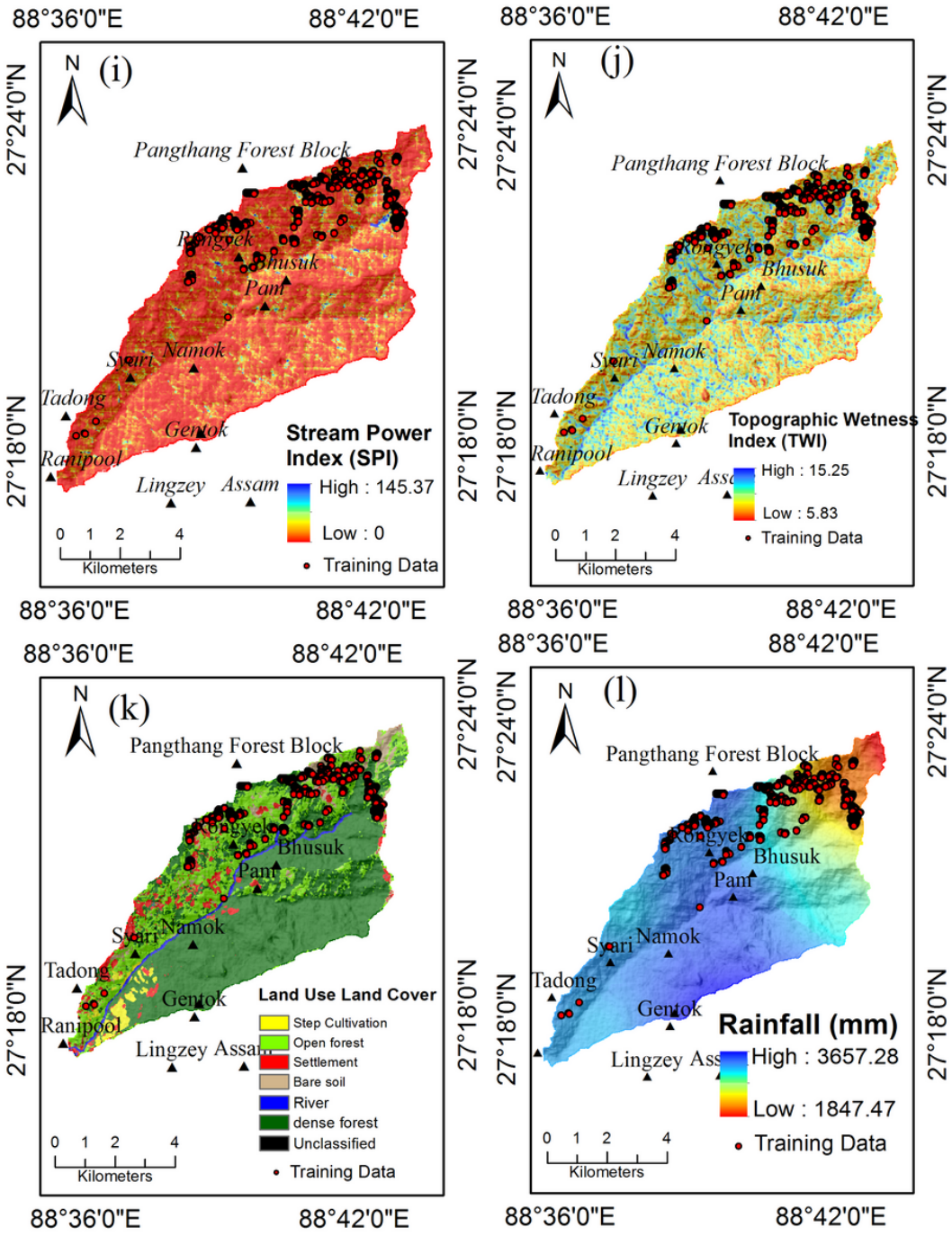

Figure 7

Landslide conditioning factors i. Stream power index (SPI) j. Topographic position index (TPI) k. Land use land cover (LULC) l. Rainfall

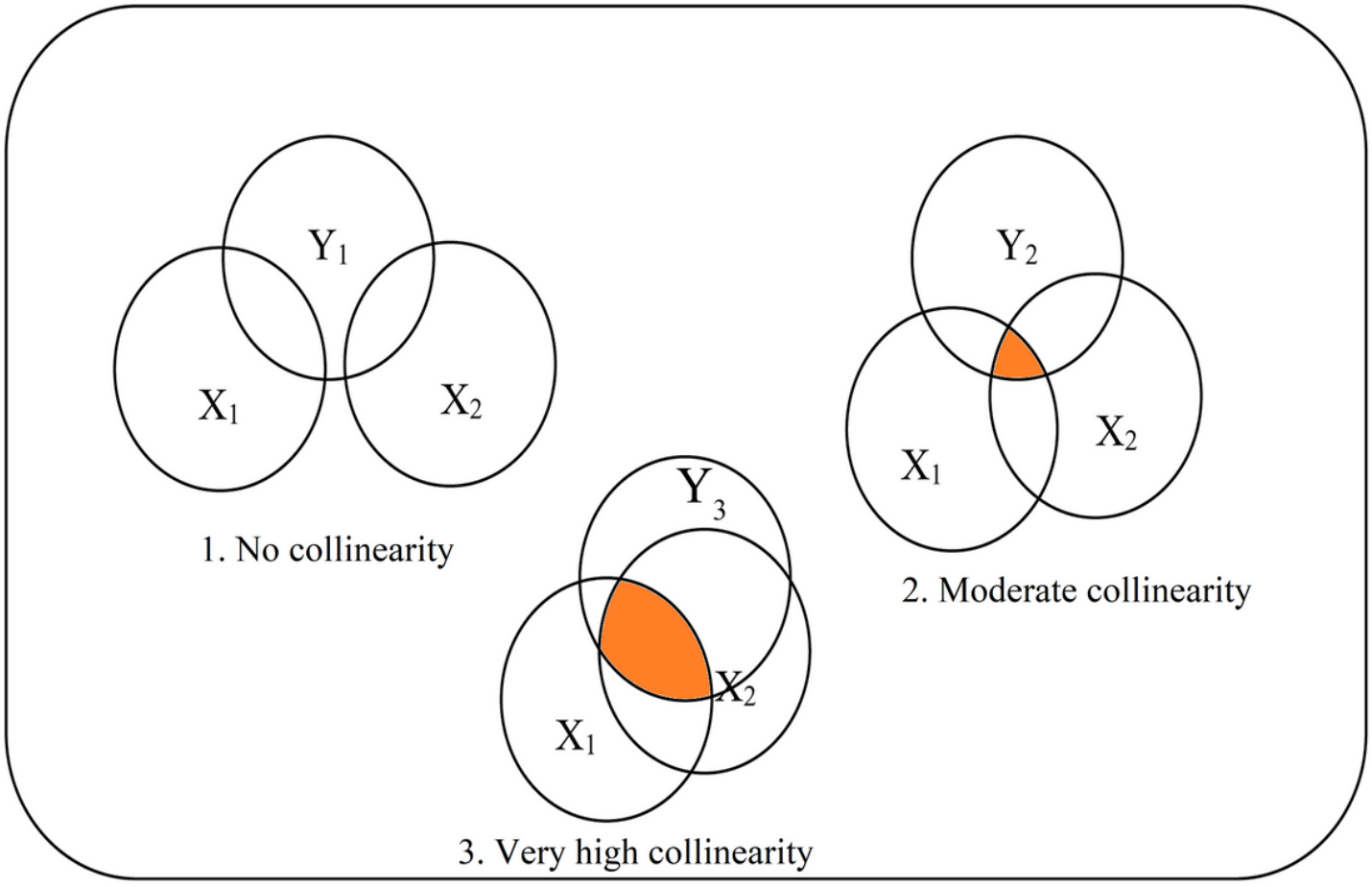

Figure 8

The conceptual framework of multicollinearity testing phenomenon showing 1. No relationship between variables, 2. Showing moderate relationship and 3. Showing very high collinearity

Image not available with this version

Figure 9

Landslide susceptibility map emanated by Bivariate Statistical Index (BSI) model

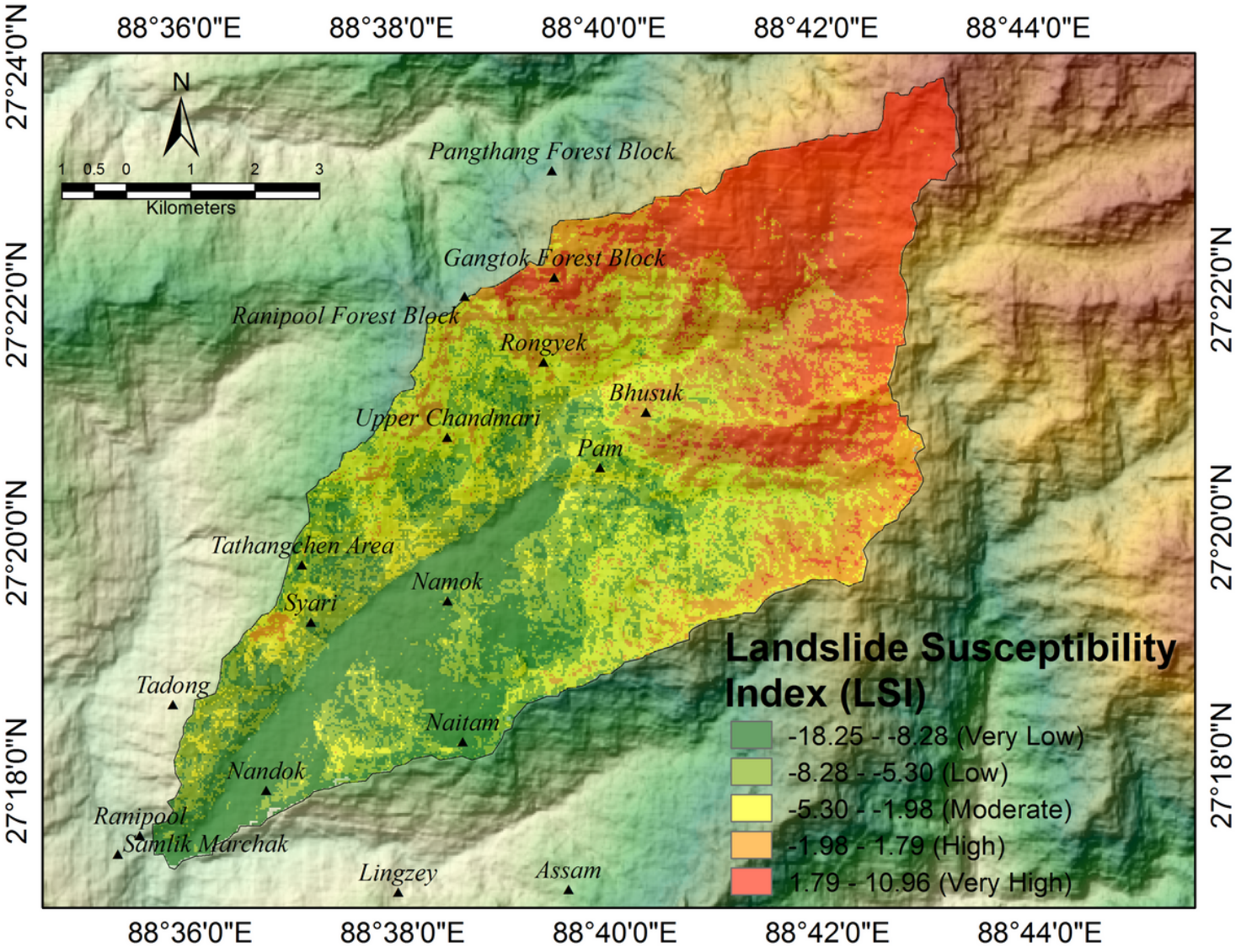

Figure 10

Landslide susceptibility map emanated by Weight of evidence (WOE) model

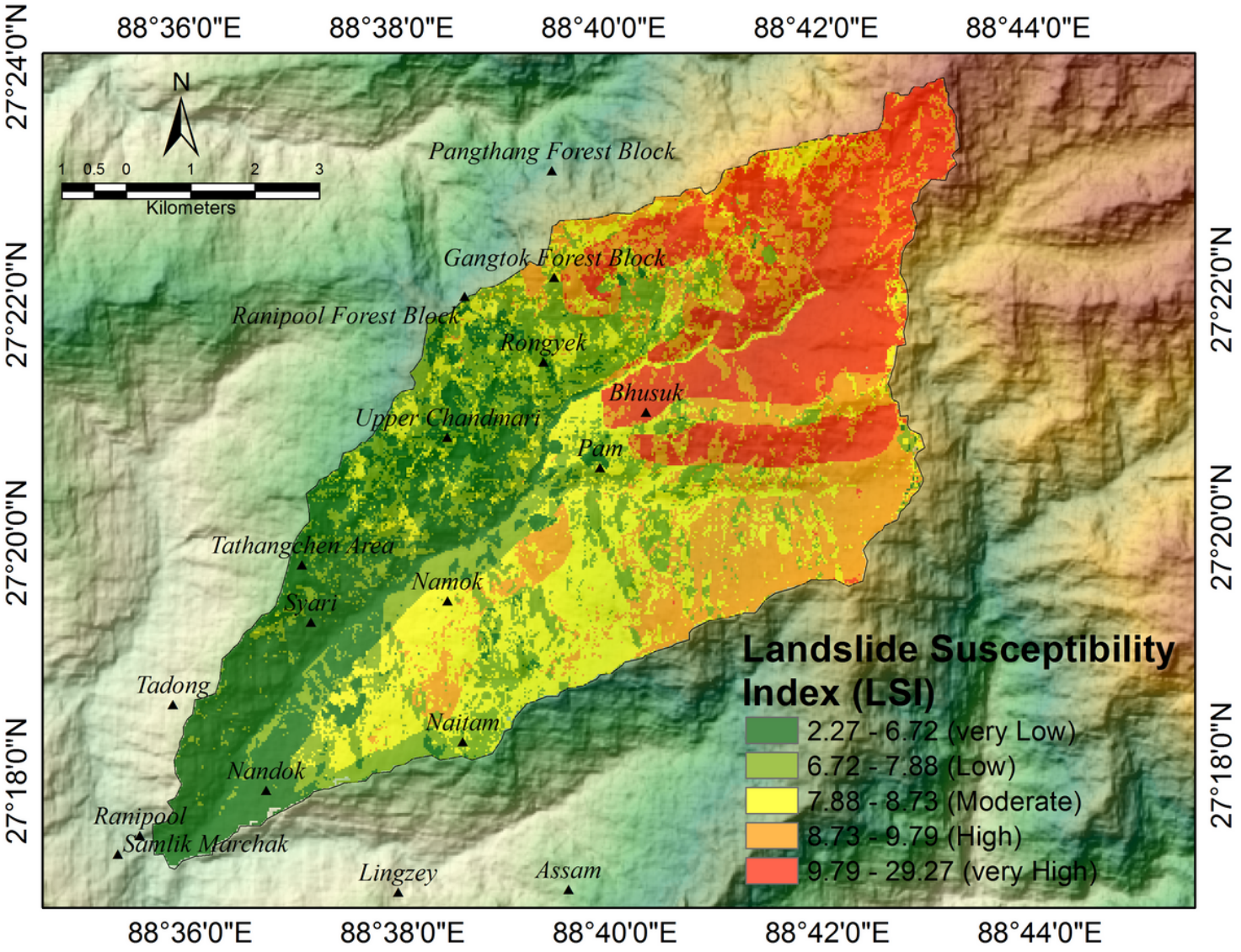

Figure 11

Landslide susceptibility map emanated by Index of Entropy (IOE) model

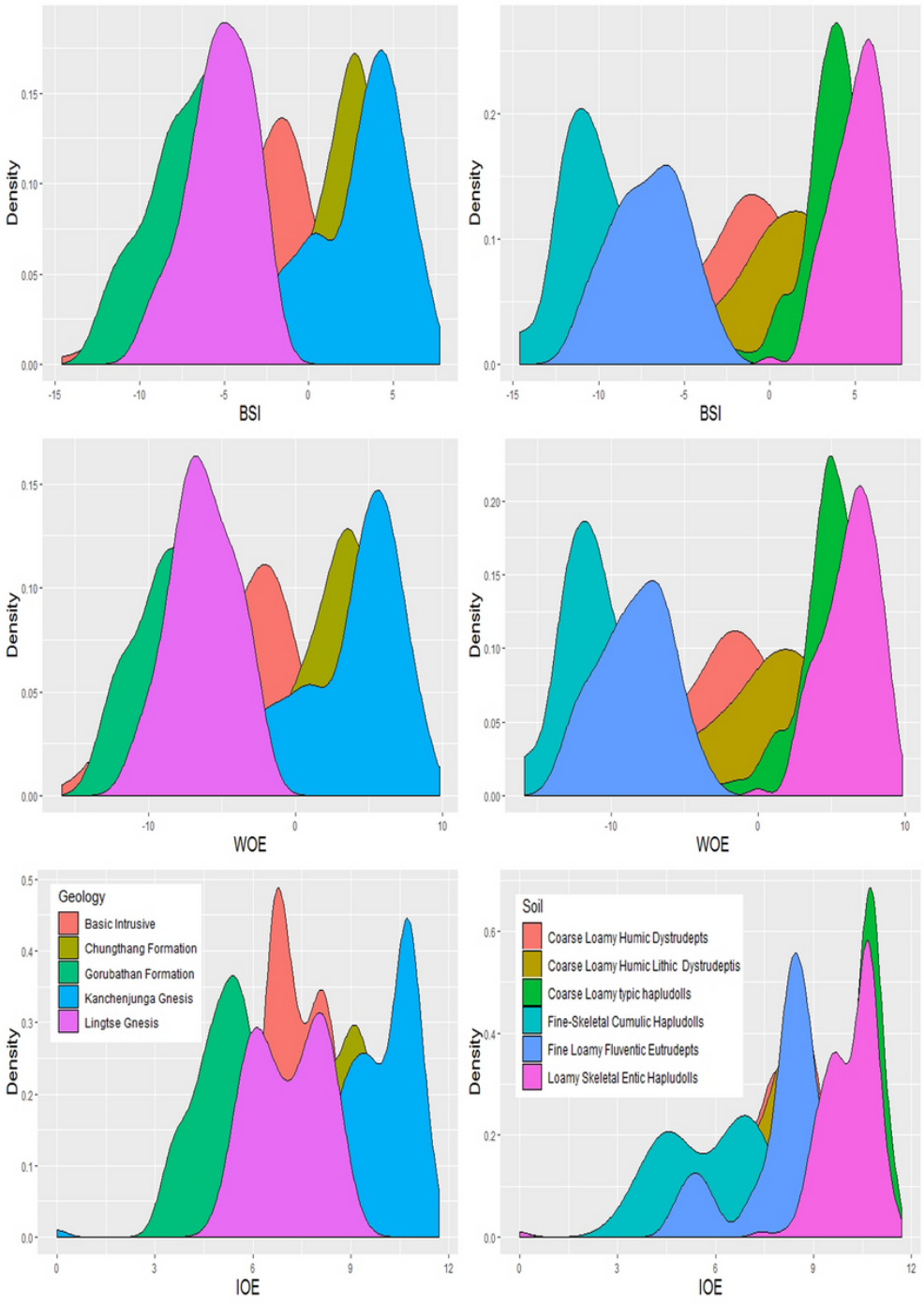

Figure 12

The relationship between different model (BSI, IOE and WOE) with the geology and soil factors of Rorachu watershed

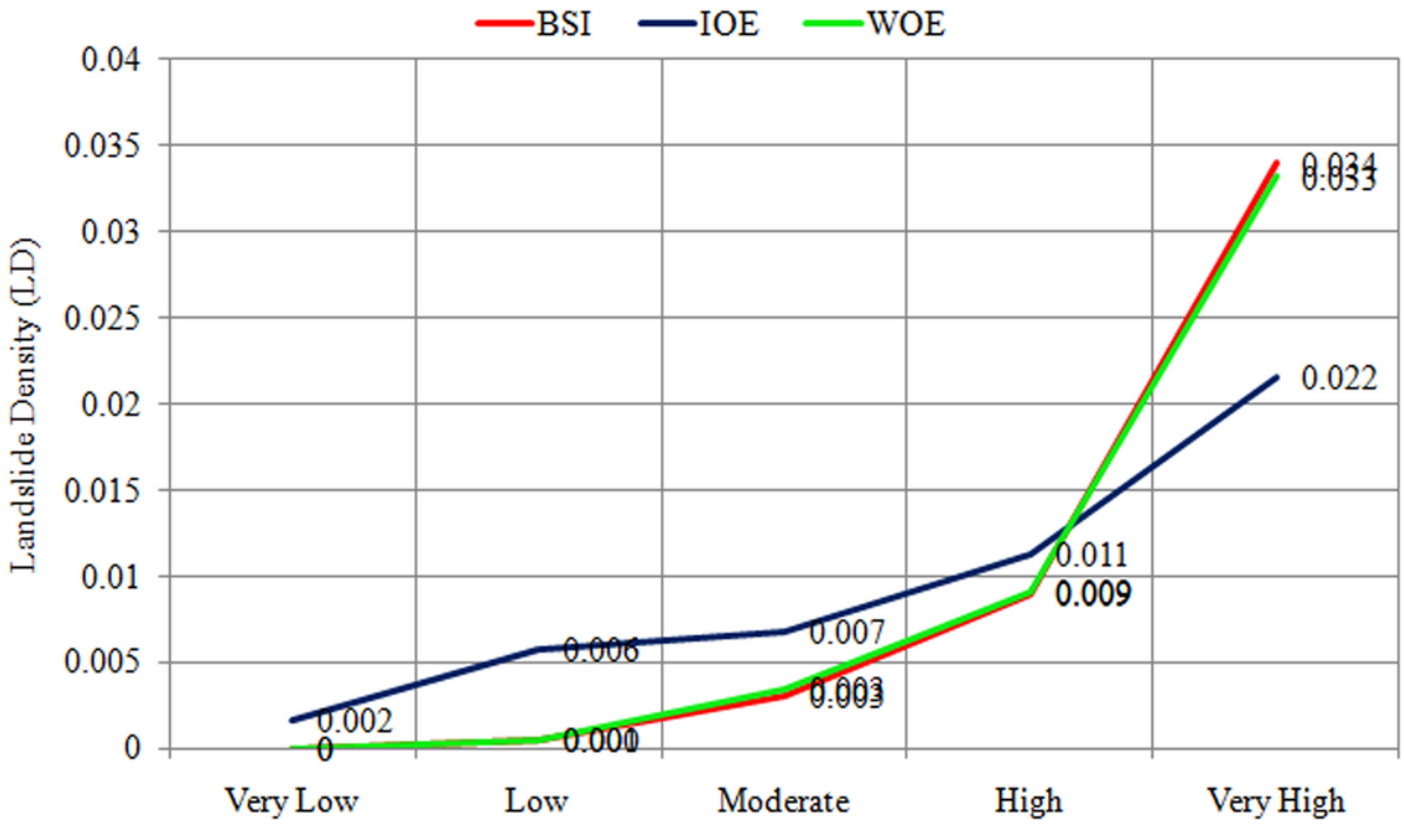

Figure 13

The landslide density of different susceptible class in the various landslide susceptibility index models (BSI, IOE and WOE).

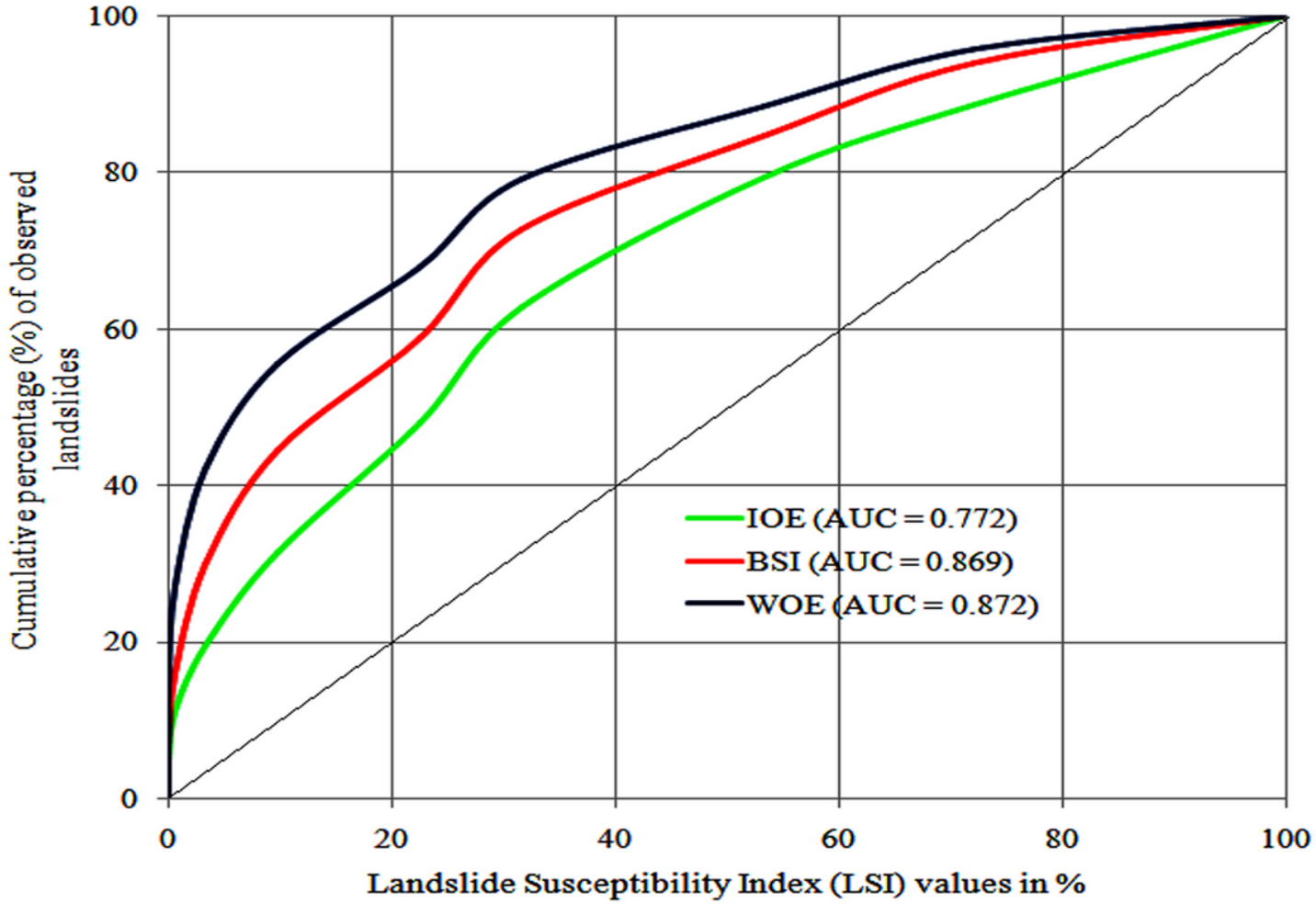

Figure 14

Success rate curve (SRC) for the three models (BSI, IOE and WOE) in the Rorochu watershed

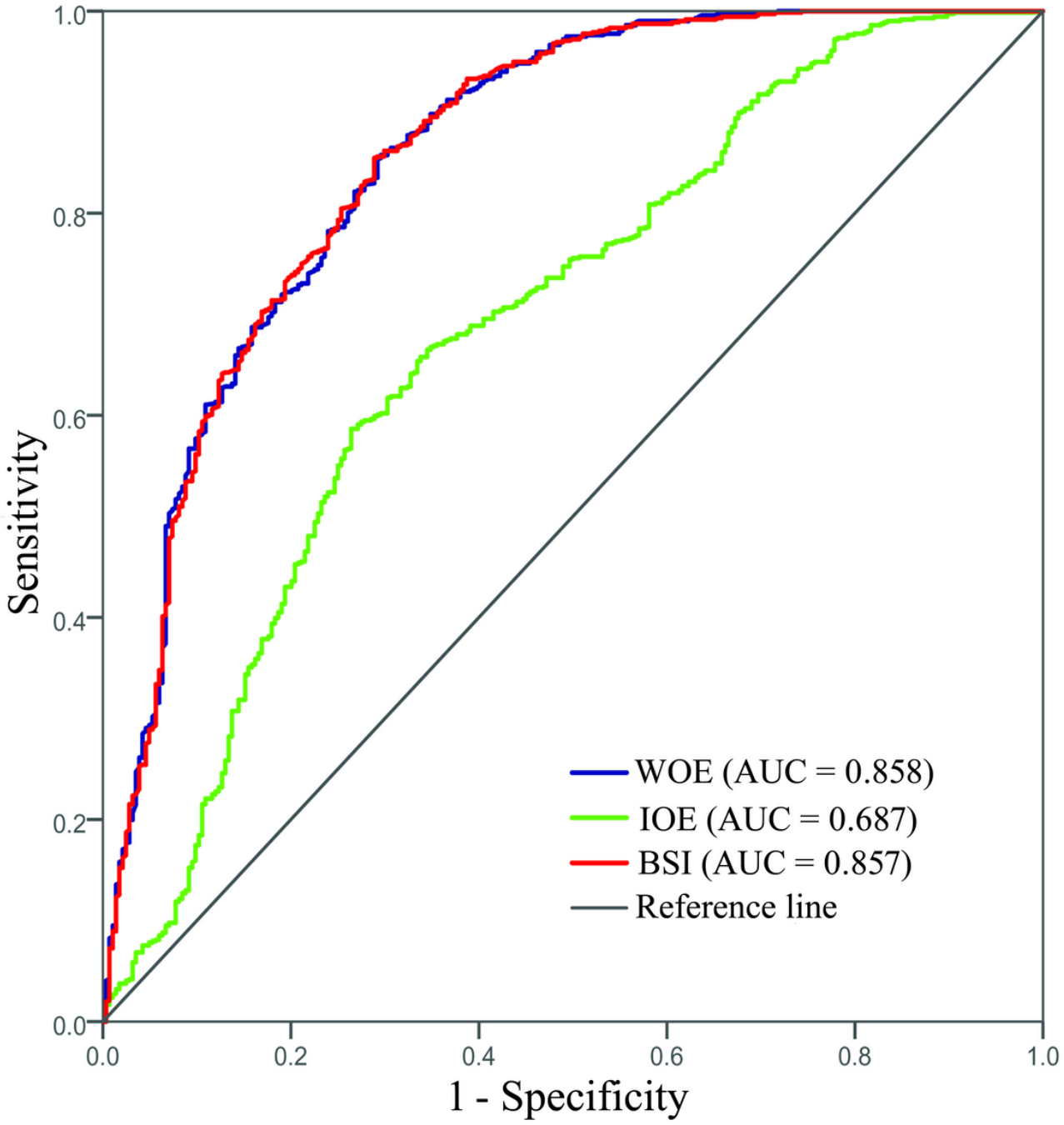

Figure 15

Receive operating characteristics (ROC) curve for Bivariate Statistical Index (BSI), Index of Entropy (IOE) and Weight of Evidence (WOE) model.

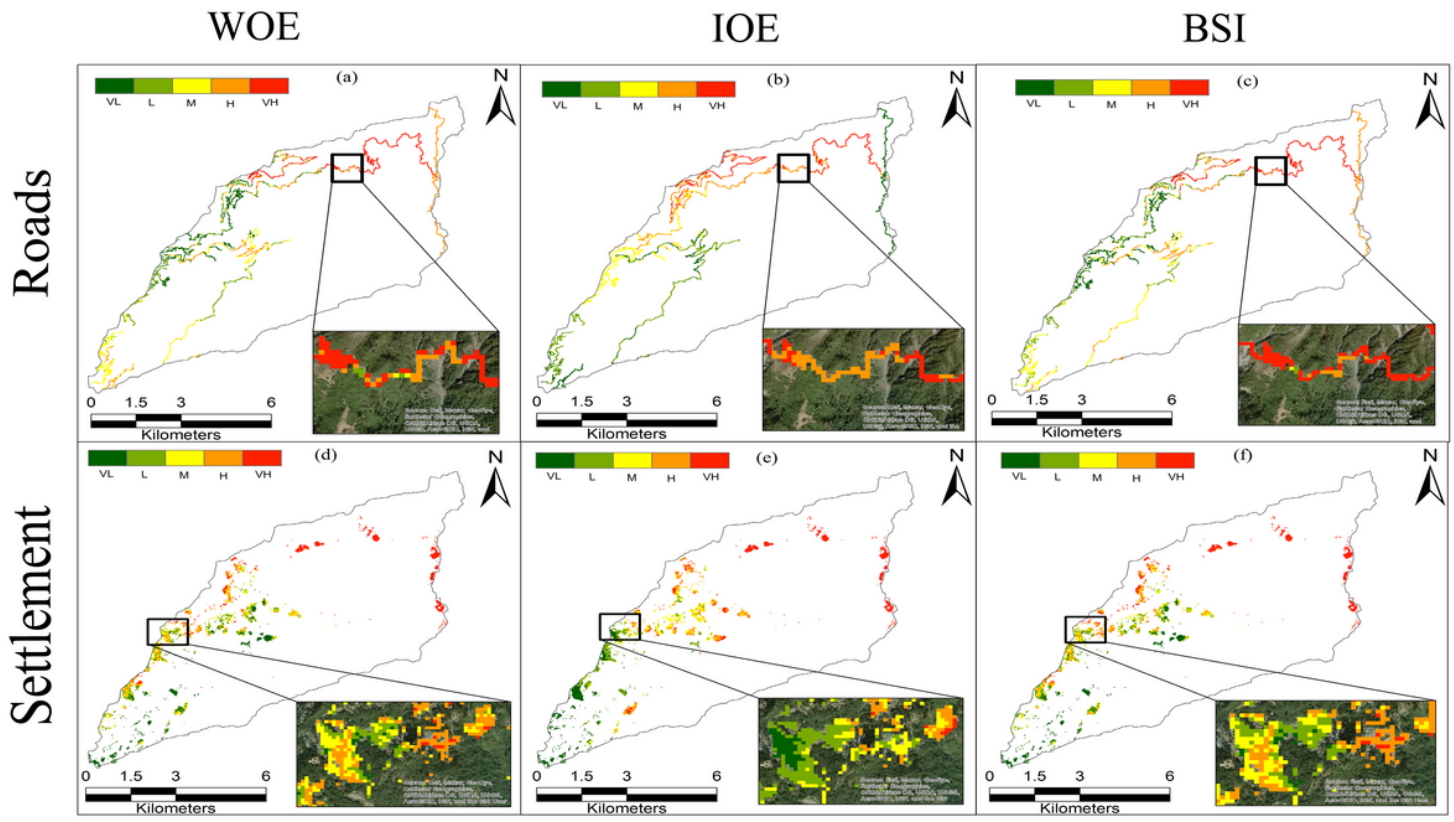

Figure 16

Landslide risk map of two variables (Settlement and Road) by the various models (a) Road risk map by Weight of Evidence (WOE) model, (b) Road risk map by Index of Entropy (IOE) model, (c) Road risk map by Bivariate Statistical Index (BSI) model, (d) Settlement risk map by Weight of Evidence (WOE) model, (e) Settlement risk map by Index of Entropy (IOE) model and (f) Settlement risk map by Bivariate Statistical Index (BSI) model

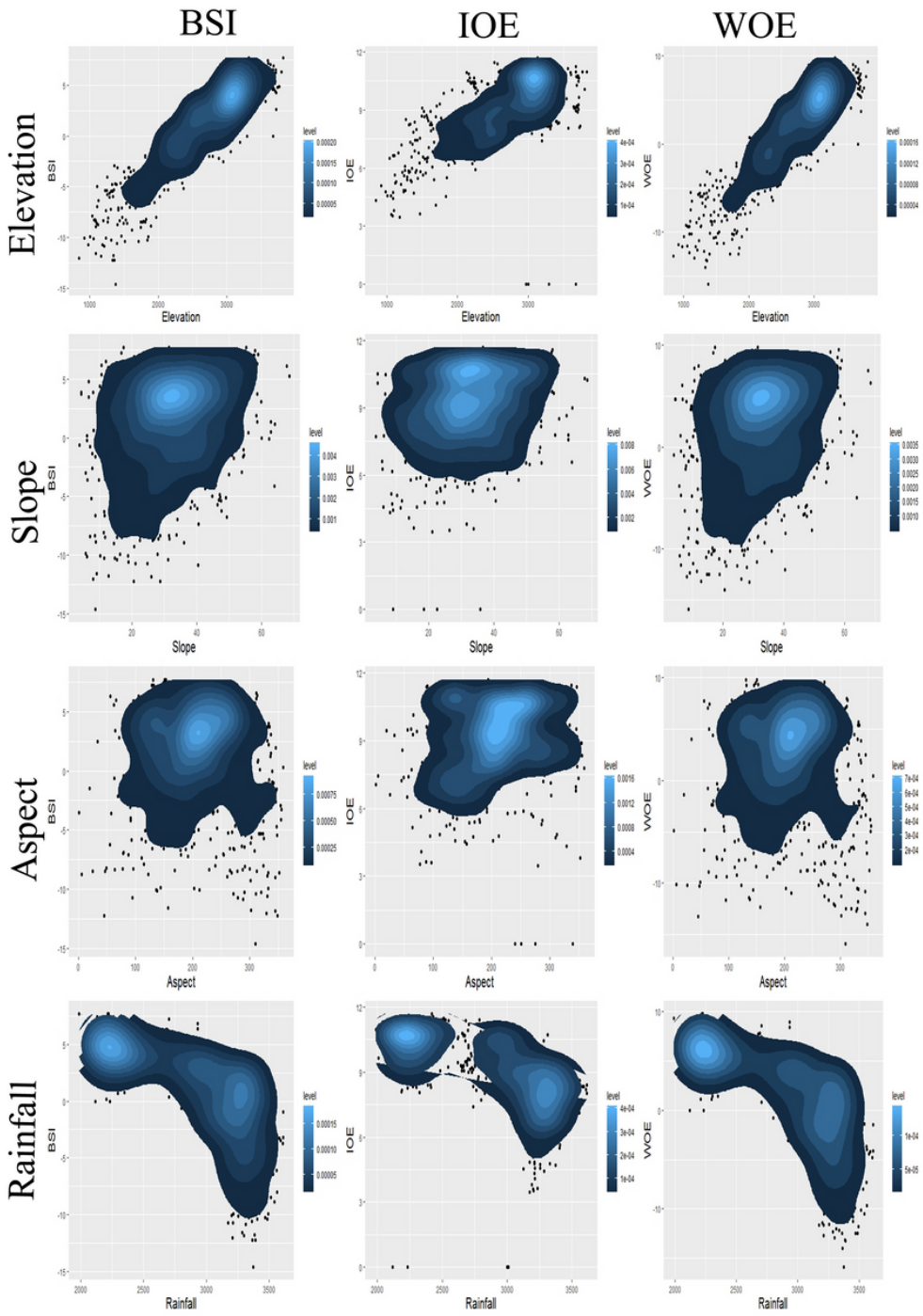

Figure 17

The correlation and density concentration between the BSI, IOE and WOE model with the Elevations, Slope, Aspect and Rainfall.